

Mads Thomassen ORCID iD: 0000-0003-0078-1217

Emma Tudini ORCID iD: 0000-0002-5834-7862

Michael Parsons ORCID iD: 0000-0003-3242-8477

Brage Andresen ORCID iD: 0000-0001-7488-3035

Rachid Karam ORCID iD: 0000-0002-5645-498X

Paul James ORCID iD: 0000-0002-4361-4657

David Goldgar ORCID iD: 0000-0003-0697-9347

Logan Walker ORCID iD: 0000-0003-0018-3719

Kathleen Claes ORCID iD: 0000-0003-0841-7372

Diana Baralle ORCID iD: 0000-0002-3560-6980

Ana Vega ORCID iD: 0000-0002-7416-5137

Maaïke Vreeswijk ORCID iD: 0000-0003-4068-9271

Miguel de la Hoya ORCID iD: 0000-0002-8113-1410

Amanda Spurdle ORCID iD: 0000-0003-1337-7897

**Clinical, splicing and functional analysis to classify *BRCA2* exon 3 variants:
application of a points-based ACMG/AMP approach**

Mads Thomassen^{*1}, Romy L.S. Mesman^{*2}, Thomas V.O. Hansen³, Mireia

Menendez⁴, Maria Rossing⁵, Ada Esteban-Sánchez⁶, Emma Tudini⁷, Therese

Törngren⁸, Michael T. Parsons⁷, Inge Sokilde Pedersen⁹⁻¹¹, Soo Hwang Teo^{12, 13},

Torben A. Kruse¹, Pål Møller¹⁴, Åke Borg⁸, Uffe Birk Jensen¹⁵, Lise Lotte

Christensen¹⁶, Christian F. Singer¹⁷, Daniela Muhr¹⁷, Marta Santamarina¹⁸⁻²⁰, Rita

Brandao²¹, Brage S. Andresen²², Bing-Jian Feng²³, Daffodil Canson⁷, Marcy E.

Richardson²⁴, Rachid Karam²⁴, Tina Pesaran²⁴, Holly LaDuca²⁴, Blair R. Conner²⁴,

This article has been accepted for publication and undergone full peer review but has not been through the copyediting, typesetting, pagination and proofreading process, which may lead to differences between this version and the Version of Record. Please cite this article as doi: 10.1002/humu.24449.

This article is protected by copyright. All rights reserved.

Nelly Abualkheir²⁴, Lily Hoang²⁴, Fabienne M.G.R. Calléja², Lesley Andrews²⁵, Paul A. James^{26, 27}, Dave Bunyan²⁸, Amanda Hamblett²⁹, Paolo Radice³⁰, David E. Goldgar²³, Logan C. Walker³¹, Christoph Engel³², Kathleen B.M. Claes³³, Eva Macháčkova³⁴, Diana Baralle²⁸, Alessandra Viel³⁵, Barbara Wappenschmidt^{36, 37}, Conxi Lazaro⁴, Ana Vega¹⁸⁻²⁰, ENIGMA Consortium, Maaïke P.G. Vreeswijk^{**2}, Miguel de la Hoya^{**6}, Amanda B. Spurdle^{**7}.

*: MT and RLSM should be considered joint first authors

** :MPGV, MdlH and ABS should be considered joint senior authors

Corresponding authors:

Mads Thomassen; Mads.Thomassen@rsyd.dk

Amanda Spurdle; Amanda.Spurdle@qimrberghofer.edu.au

¹ Department of Clinical Genetics, Odense University Hospital, Odense C, Denmark.

² Department of Human Genetics, Leiden University Medical Center, Leiden, The Netherlands.

³ Department of Clinical Genetics, Rigshospitalet, Copenhagen University Hospital, Copenhagen, Denmark.

⁴ Hereditary Cancer Program, "Catalan Institute of Oncology, ONCOBELL-IDIBELL-IDTP, CIBERONC", 08908 Hospitalet de Llobregat, Spain.

⁵ Center for Genomic Medicine, Rigshospitalet, Copenhagen University Hospital, Copenhagen, Denmark.

⁶ Molecular Oncology Laboratory, CIBERONC, Hospital Clinico San Carlos, IdISSC (Instituto de Investigación Sanitaria del Hospital Clínico San Carlos), Madrid, Spain.

⁷ Department of Genetics and Computational Biology, QIMR Berghofer Medical Research Institute, Brisbane, Queensland, Australia.

⁸ “Division of Oncology, Department of Clinical Sciences Lund”, Lund University, Lund, Sweden.

⁹ Molecular Diagnostics, Aalborg University Hospital, Aalborg, Denmark.

¹⁰ Clinical Cancer Research Center, Aalborg University Hospital, Aalborg, Denmark.

¹¹ Department of Clinical Medicine, Aalborg University, Aalborg, Denmark.

¹² Breast Cancer Research Programme, Cancer Research Malaysia, Subang Jaya, Selangor, Malaysia.

¹³ Department of Surgery, Faculty of Medicine, University of Malaya, Kuala Lumpur, Malaysia.

¹⁴ Department of Tumour Biology, “The Norwegian Radium Hospital, Oslo University Hospital”, Oslo, Norway.

¹⁵ Department of Clinical Genetics, Aarhus University Hospital, Aarhus N, Denmark.

¹⁶ Division of Surgical Oncology, National Cancer Centre, Singapore, Singapore.

¹⁷ Dept of OB/GYN and Comprehensive Cancer Center, Medical University of Vienna, Vienna, Austria.

¹⁸ Fundación Pública Galega de Medicina Xenómica, Santiago de Compostela, Spain.

¹⁹ Instituto de Investigación Sanitaria de Santiago de Compostela (IDIS), Complejo Hospitalario Universitario de Santiago, SERGAS, Santiago de Compostela, Spain.

²⁰ Centro de Investigación en Red de Enfermedades Raras (CIBERER), Madrid, Spain.

²¹ Department of Clinical Genetics, Maastricht University Medical Center, Maastricht, The Netherlands.

²² Departmen of Biochemistry and Molecular Biology and the Villum Center for Bioanalytical Sciences, University of Southern Denmark, 5230 Odense, Denmark.

²³ Department of Dermatology, Huntsman Cancer Institute, University of Utah School of Medicine, Salt Lake City, UT, USA.

²⁴ Ambry Genetics, “Aliso Viejo, CA”, USA.

²⁵ Hereditary Cancer Clinic, Nelune Comprehensive Cancer Care Centre, Randwick, New South Wales, Australia.

²⁶ Parkville Familial Cancer Centre, Peter MacCallum Cancer Center, Melbourne, Victoria, Australia.

²⁷ Sir Peter MacCallum Department of Oncology, The University of Melbourne, Melbourne, Victoria, Australia.

²⁸ “Human Development and Health, Faculty of Medicine”, University of Southampton, Southampton, UK.

²⁹ Middlesex Health Shoreline Cancer Center, Westbrook, CT, USA.

³⁰ Unit of Molecular Bases of Genetic Risk and Genetic Testing, Department of Research, Fondazione IRCCS Istituto Nazionale dei Tumori (INT), Milan, Italy.

³¹ Department of Pathology and Biomedical Science, University of Otago, Christchurch, New Zealand.

³² Institute for Medical Informatics, Statistics and Epidemiology, University of Leipzig, Leipzig, Germany.

³³ Centre for Medical Genetics, Ghent University, Gent, Belgium.

³⁴ Department of Cancer Epidemiology and Genetics, Masaryk Memorial Cancer Institute, Brno, Czech Republic.

³⁵ Division of Functional onco-genomics and genetics, Centro di Riferimento Oncologico di Aviano (CRO), IRCCS, Aviano, Italy.

³⁶ Center for Familial Breast and Ovarian Cancer, Faculty of Medicine and University Hospital Cologne, University of Cologne, Cologne, Germany.

³⁷ Center for Integrated Oncology (CIO), Faculty of Medicine and University Hospital Cologne, University of Cologne, Cologne, Germany.

Grant support: The work of MPG V was financially supported by the Dutch Cancer Society KWF (UL2012-5649 and Pink Ribbon-11704). The work by PM was supported by a “Pink ribbon” grant #194751 from Den Norske Kreftforening to E.H. The work of MdIH was supported by Spanish Instituto de Salud Carlos III (ISCIII) funding grant PI 20/00110, an initiative of the Spanish Ministry of Economy and Innovation. ABS, MTP and ET were supported by NHMRC Funding (APP177524, APP1104808). The work by CL and MM received institutional support by CERCA Program/ Generalitat de Catalunya and grant support by the Carlos III National Health Institute funded by FEDER funds – a way to build Europe – [PI19/00553; PI16/00563; SAF2015-68016-R and CIBERONC]; the Government of Catalonia [Pla estratègic de recerca i innovació en salut (PERIS_MedPerCan and URDCat projects), 2017SGR1282 and 2017SGR496]. The Baralle lab is supported by NIHR Research Professorship to DB (RP-2016-07- 011). The work of AV was supported by the Spanish Health Research Foundation, Instituto de Salud Carlos III (ISCIII) through Research Activity Intensification Program (contract grant numbers: INT15/00070, INT16/00154, INT17/00133, INT20/00071), and through Centro de Investigación Biomédica en Red de Enfermedades Raras CIBERER (ACCI 2016: ER17P1AC7112/2018); Autonomous Government of Galicia (Consolidation and structuring program: IN607B), and by the Fundación Mutua Madrileña (call 2018). The German Consortium of Hereditary Breast and Ovarian Cancer (GC-HBOC) is supported by the German Cancer Aid (grant no 110837 and 70114178), (RKS) and by the Federal Ministry of Education and Research (grant no 01GY1901), (RKS). The work of EMA was Supported by Ministry of Health of the Czech Republic

MH CZ – DRO (MMCI, 00209805) and AZV project NU20-03-00285. Institutional support by Italian Ministry of Health, Ricerca Corrente of CRO Aviano, Line 1 (AVI).

Abstract

Skipping of *BRCA2* exon 3 ($\Delta E3$) is a naturally occurring splice event, complicating clinical classification of variants that may alter $\Delta E3$ expression. This study used multiple evidence types to assess pathogenicity of 85 variants in/near *BRCA2* exon 3. Bioinformatically predicted spliceogenic variants underwent mRNA splicing analysis using minigenes and/or patient samples. $\Delta E3$ was measured using quantitative analysis. A mouse embryonic stem cell (mESC) based assay was used to determine the impact of 18 variants on mRNA splicing and protein function. For each variant, population frequency, bioinformatic predictions, clinical data and existing mRNA splicing and functional results were collated. Variant class was assigned using a gene-specific adaptation of ACMG/AMP guidelines, following a recently proposed points-based system. mRNA and mESC analysis combined identified six variants with transcript and/or functional profiles interpreted as loss of function. Cryptic splice site use for acceptor site variants generated a transcript encoding a shorter protein that retains activity. Overall, 69/85 (81%) variants were classified using the point-based approach. Our analysis shows the value of applying gene-specific ACMG/AMP guidelines using a points-based approach and highlights the consideration of cryptic splice site usage to appropriately assign PVS1 code strength.

Keywords: *BRCA2*, Splicing, ACMG/AMP classification, mESC, dPCR, quantitation

Introduction

Pathogenic variants in *BRCA2* predispose carriers to breast, ovarian, prostate and other *BRCA2*-related cancers (Gayther et al., 1997). Although intensive gene testing has been performed for families with suspected hereditary cancer for more than 20 years, there are still considerable challenges for the interpretation of variants with uncertain clinical significance (Spurdle et al., 2012). Several naturally occurring alternative splice isoforms of *BRCA2* have been reported, and genetic variants have been shown to change the relative expression levels of these alternative transcripts (de Garibay et al., 2014; Fackenthal et al., 2016; Montalban et al., 2018). Interpretation of clinical significance for these spliceogenic variants is difficult as aberrant transcript expression patterns might impact protein function depending on both transcript ratios and the functional integrity of the alternative isoforms. Skipping of *BRCA2* exon 3 ($\Delta E3$) is a naturally occurring in-frame splicing event (Peixoto et al., 2009; Thomassen et al., 2012). Several genetic variants have been shown to increase $\Delta E3$ at the mRNA level (Caputo et al., 2018; Diez et al., 2007), and there is now convincing evidence that near exclusive expression of the $\Delta E3$ transcript (also termed complete exon skipping, or complete $\Delta E3$) is deleterious to protein function and confers high risk of *BRCA2*-related cancers (Caputo et al., 2018). The *BRCA2* protein is, through interactions with several other proteins including *BRCA1* and *PALB2*, involved in the repair of DNA double-strand breaks (DSB) by homologous recombination (Sy, et al., 2009). Exon 3 encodes the *PALB2* interaction domain located at amino acids 21-39 (Oliver et al., 2009), and abrogation of *BRCA2*-*PALB2* binding is the likely molecular mechanism underlying this increased risk (Hartford et

al., 2016). In contrast, the *BRCA2* c.68-7T>A variant (Colombo et al., 2018) leads to moderately increased $\Delta E3$ relative to wildtype (WT) levels (13% $\Delta E3$, compared to 3% in non-carriers in lymphoblastoid cell line (LCL) cultures, inferring 23% $\Delta E3$ expression from the A allele), but this variant is not associated with elevated breast cancer risk. A more recent analysis (Tubeuf et al., 2020) reported that a common synonymous variant c.231T>G rescued *BRCA2* function in a mouse embryonic stem cell (mESC) complementation assay, with the G allele reported to exhibit 32-40% $\Delta E3$ in the mESC assay and 30% $\Delta E3$ in a minigene assay. These findings suggested that moderately increased $\Delta E3$ expression is not associated with high risk of cancer, complicating the clinical interpretation of variants that affect mRNA splicing in this region of the gene.

In this study, we assessed the pathogenicity of 85 variants located in or near *BRCA2* exon 3, using a variety of evidence types. These included new and existing data from mRNA and/or protein/cellular functional assays, frequency and bioinformatic data calibrated against clinical data, and additional likelihood-weighted clinical evidence. We show the value of applying gene-specific ACMG/AMP guidelines. In particular, this study provides real-world examples to demonstrate the flexibility of the recently proposed points-based approach (Tavtigian et al., 2020) to resolve variant interpretations.

Materials and Methods

The overall project, using de-identified data and laboratory results collated from multiple sites, was approved by the QIMR Berghofer Human Research Ethics

Committee (Project 1051). Each participating site had Human Research Ethical Approval to cover use of patient material and data in research to evaluate variant pathogenicity, including: Ethical committee in Region of Southern Denmark and Capital Region of Denmark, approval VF20050011 and H-18058595, respectively (MT, MR); IdISSC/HCSC Ethics Committee, Project 15/139-E_BS and 21/308-E (Mdelah); Ethical committee of the Masaryk Memorial Cancer Institute (approval 2019/1845/MMCI: project NU20-03-00285) (EMA); IRB numbers EK-Nr 056/2005 and 2190/2019 from the Medical University of Vienna, IRB (CSI); The ethical committee at Lund University Dnr 2011/349 2011/652 (AB); Ethical Territorial Committee Research of Santiago Lugo, approval 2018/200 (AV); Ethics Committee of the University of Cologne (TEMP991529 and 19-1360_4) (BW); CRO Aviano, Local Ethical Committee, approval CRO-15-1997 (AVI) and IRB number IRAS ID 49685 (DB); Ethics committee of Bellvitge Biomedical Research Institute (IDIBELL; PR278/19 (MM). Use of the Ambry de-identified dataset for research was deemed exempt from review by the Western Institutional Review Board.

BRCA2 Exon 3 Variants

A total of 89 variants were included in the study. Four previously classified variants with quantified splicing alterations were used as controls: Two variants were known to cause complete $\Delta E3$ (Caputo et al., 2018) and previously confirmed to be associated with *BRCA2*-related clinical phenotypes (c.156_157insAlu; c.316+5G>C); variant c.68-7T>A was included as a “partial skipping” control classified on the basis of clinical information as benign (Colombo et al., 2018);

common synonymous variant c.231T>G, previously reported to exhibit at least 30% Δ E3 and also to rescue BRCA2 function in a mESC complementation assay (Tubeuf et al., 2020), was included as an mESC experimental control and was considered benign based on frequency. An additional variant was included as an experimental control: Variant c.316+5G>A, previously shown to lead to complete Δ E3 but not formally classified using clinical data (Caputo et al., 2018). Through examination of the literature, and/or by communication with ENIGMA members additional variants in exon 3 and the flanking introns were identified for inclusion in the study (Supplementary Table 1). For completeness, additional single nucleotide substitutions at the exon 3 acceptor site were included in minigene assays. In addition, four predicted missense substitution variants (c.91T>C p.(Trp31Arg), c.91T>G p.(Trp31Gly), c.93G>C p.(Trp31Cys) and c.93G>T p.(Trp31Cys)) were included in the mESC assay due to their location in the region relevant for BRCA2-PALB2 protein interaction (Oliver et al., 2009), and previous reports of variant impact on Δ E3 for c.93G>T (Biswas et al., 2012; Sanz et al., 2010)(Sharan, personal communication).

Most variants had been identified in families with suspicion of hereditary breast and/or ovarian cancer. Overall, in addition to the controls with confirmed pathogenicity (pathogenic controls c.156_157insAlu, c.316+5G>C; benign controls c.68-7T>A and common synonymous variant c.231T>G), bioinformatic, mRNA, functional, and clinical data were collated for another 85 variants from the literature and/or as part of this study - including experimental control c.316+5G>A.

BRCA2 variants and alternative splicing events were described according to recommendations from the Human Genome Variant Society (HGVS) (<http://varnomen.hgvs.org/>), using as a reference the Refseq transcript NM_000059.3. For the sake of simplicity, we identified events as well with a code that combines the following symbols: Δ (skipping of reference exonic sequences), ∇ (inclusion of reference intronic sequences), p (acceptor shift) and, q (donor shift). When necessary, the exact number of nucleotides skipped (or retained) is indicated.

Initial bioinformatic prediction to prioritize variants for mRNA assays, was performed using MaxEntScan and ESEfinder software implemented in AlamutVisual 2.15 (<https://www.interactive-biosoftware.com>) (Supplementary Table 1). See section “Variant classification, bioinformatics-based codes” for details on additional predictions used for comparison to mRNA findings and for variant interpretation.

Laboratory analyses

Primers and methods used for mRNA assays are provided in Supplementary Table 2.

Splicing analysis of patient samples and minigene assays:

At study initiation, variants identified from ENIGMA collaborators to have bioinformatic prediction of altered splicing were prioritized for minigene assays and/or analysis of patient samples if available. Additional variants were included on the basis of mRNA availability only. Details on bioinformatics score and rationale for mRNA analysis are included in Supplementary Table 1. In total, excluding control variants, minigene assays were performed for 21 unique variants, and splicing

assays on patient mRNA were performed across multiple labs for 14 unique variants. The patient samples were originally either sampled directly in RNA stabilizing agents (PAXgene® tubes and Tempus® tubes), or lymphocytes were grown as either short term cultures or long term EBV-transformed lymphoblastoid cell lines (LCLs). In order to detect splicing alterations in addition to $\Delta E3$ with high sensitivity, capillary gel electrophoresis was applied for 11 variants using methods described previously (de la Hoya et al., 2016). During the course of the study, published mRNA splicing results for these and additional variants in/near exon 3 were also collated.

Quantitation of splice events by digital PCR:

The use of digital PCR (dPCR) for precise quantification of *BRCA2* alternatively spliced isoforms has been described in detail elsewhere (Colombo et al., 2018). In brief, dPCR experiments were performed on a QuantStudio 3D dPCR 20K platform according to the manufacturer's instructions (Applied Biosystems, Foster City, CA). All quantification experiments were performed combining FAM and VIC labelled TaqMan assays (Applied Biosystems, Foster City, CA) in individual chips. Chips were analyzed in the QuantStudio 3D Analysis Suit Cloud software v2.0 (Applied Biosystems, FosterCity, CA), defining FAM as the target. Default settings were used in all cases. After reviewing automatic assessment of the chip quality by the software, only green flag chips (data met all quality thresholds, review of the analysis result not required) and yellow flag chips (data met all quality thresholds, but manual inspection is recommended) were considered for further analyses. To

detect *BRCA2* $\Delta E3$ we used a FAM-labeled custom designed TaqMan assay (Applied Biosystems) specific for the *BRCA2* exon 2-4 junction. *BRCA2* exon 3 retention was detected with a VIC-labeled Hs01556199 assay (Applied Biosystems) specific for the *BRCA2* exon 3-4 junction. $\Delta E3$ level was calculated as $\text{exon 2-4}/(\text{exon 2-4} + \text{exon 3-4})$. Note that, the latter assay will recognize different transcripts, provided that they have a native exon 3-4 junction i.e., the assay does not discriminate full-length expression from expression of transcripts with alterations at the exon 2-exon 3 junction, such as $\Delta E3p6$ or $\nabla E3p2$.

To better compare results using patient mRNA (where naturally occurring exon 3 skipping from the WT allele has to be accounted for) with data from assays measuring the effect of a single allele (i.e., minigene and mESC assay), the results were presented as absolute $\Delta E3$ level, and additionally as inferred per-allele $\Delta E3$ level, calculated as follows: two times $\Delta E3$ exclusion level observed in carriers minus the WT $\Delta E3$ level (from same sample type).

Furthermore, the level of two other naturally occurring *BRCA2* alternative splicing isoforms ($\Delta E3-E4$ and $\Delta E3-E7$) skipping exon 3 (Fackenthal et al., 2016) were measured using FAM-labeled custom designed TaqMan assay (Applied Biosystems) specific for the *BRCA2* exon 2-5 and exon 2-8 junctions, respectively. Full-length *BRCA2* transcript was detected with a VIC-labeled Hs00609073_m1 assay (Applied Biosystems) specific for the *BRCA2* exon 26-27 junction. Exclusion levels were calculated as $\text{exon 2-X}/(\text{exon 2-X} + \text{exon 26-27})$ where X refers to exon 5 or 8. Sequences of the Taqman probes are in Supplementary Table 2.

RNA Sequencing:

Paired germline DNA-RNA genetic testing at Ambry Genetics, conducted on RNA isolated from blood collected in PaxGene tubes as described previously (Conner et al., 2019; Farber-Katz et al., 2018; Landrith et al., 2020), was performed for patients carrying *BRCA2* c.68-1G>A, c.68-2A>G and c.68-3T>G. Additional RNA-sequencing was performed to confirm percent spliced in (PSI) of the observed transcripts i.e. exon-inclusion ratio. The SuperScript™ IV One-Step RT-PCR System (Thermo Fisher Scientific, Waltham, USA) was used to reverse transcribe and amplify 500ng total RNA (see Supplementary Table 2 for details of primers). Thirty-five amplification cycles were performed with an annealing temperature of 52 °C and a 45s extension. Amplicons were purified using Ampure XP beads (Beckman Coulter, Brea, USA) and quantified using the TapeStation D1000 system (Agilent, Santa Clara, USA). An input of 125ng was used for preparation of Illumina dual indexed libraries using the Kapa HyperPrep kit with PCR (Roche, Basel, Switzerland), using 10 cycles of library amplification and a Covaris shearing protocol optimized to yield 300 bp fragments. Resulting libraries were pooled at equal molarities and sequenced using 150 bp paired-end reads on the Miseq platform (illumina, San Diego, USA). A custom bioinformatics pipeline was used to align resulting reads and calculate PSI as described previously (Landrith et al., 2020).

mESC functional assay:

In this assay, variants are introduced in the full-length human *BRCA2* gene located on a Bacterial Artificial Chromosome (BAC) and subsequently transfected in a

hemizygous mouse *Brca2* mESC line (Supplementary Figure 1) as described previously (Mesman et al., 2020). As BRCA2 protein activity is essential for mESC viability, the capacity of variants to rescue the lethal phenotype after removal of the conditional *mBrca2* allele can be used as a measure of variant protein function. Variants that severely impede cell viability are considered loss of function variants, while variants that rescue cell lethality to a certain extent can be characterized by their effect on homology directed repair (HDR) in an additional functional assay. In a previous validation study, using variants of known pathogenicity as determined by multifactorial likelihood analysis, (likely) pathogenic missense variants were either unable to rescue the lethal cell phenotype upon *mBrca2* loss or displayed an HDR level below 30% of WT BRCA2, while (likely) benign missense variants complemented the lethal phenotype and displayed HDR capacities between 50 and 120% of WT BRCA2 activity (Mesman et al., 2019). In this study, we introduced clone counting to stratify complementation categories.

The conditional *mBrca2* allele was removed by treating the cells with 1.0 μ M 4-Hydroxytamoxifen (4-OHT) (Sigma Aldrich Merck KGaA, Darmstadt, Germany) as described previously (Mesman et al., 2020). For each variant, the number of viable clones was compared to the complementation of WT BRCA2 expressing cells, and categorized in one of the following complementation categories: poor (<20% viability, including no complementation), reduced (20-50% viability) or good (>50% viability). Variants in the last two categories were included in downstream functional analysis, using the DR-GFP reporter assay to measure variant capacity to repair an I-sce1 induced DSB, which leads to the restoration of a GFP gene construct

(Mesman et al., 2020). The HDR activity for a variant was measured as the percentage of mCherry and GFP double positive cells relative to the number of double positive cells observed for WT BRCA2. For the DR-GFP reporter assay, all cell lines were seeded in triplicate, resulting in six GFP measurements per variant.

In addition to control variants c.68-7T>A, c.316+5G>C and c.231T>G, 18 variants were selected for the mESC functional assay based on observation of increased $\Delta E3$ or other aberrant splicing product detected by analysis of patient samples, minigene, or if the variant was predicted to (also) result in an amino acid change within the BRCA2-PALB2 interaction domain.

To study the effect of a variant on mRNA splicing, RNA was isolated from duplicate variant-expressing mESC using a Trizol based protocol. The dPCR method (described above) was applied on these RNA samples to analyse splicing patterns and quantify $\Delta E3$ level. Capillary gel electrophoresis (described above) was also applied for variants c.68-2A>G and c.68-3T>G.

BRCA2 protein expression in BAC-transfected mESC was confirmed by western blot analysis using a rabbit polyclonal antibody (BETHYL, A303–434A-T) directed against a region between amino acids 450–500 in exon 10 of BRCA2, as described previously (Mesman et al., 2020).

Variant classification

Variant classification was based on a gene-specific adaptation of the original ACMG/AMP guidelines (Richards et al., 2015), incorporating clinical, splicing and functional information from multiple sources, and also bioinformatic-based and frequency-based codes with weights determined from empirical data. Requests

were made to the ENIGMA membership via email for clinical information from variant carriers, including pedigree data and breast tumor histopathology status. Additional clinical, splicing and functional data were sought from publications.

Frequency-based codes

The applicable PM2 code strength was determined using the approach as described previously (Parsons et al., 2019). The likelihood ratio (LR) towards pathogenicity was estimated based on maximum population allele frequency for a set of 749 *BRCA1* and *BRCA2* variants that have previously been classified as (likely) benign or (likely) pathogenic using multifactorial likelihood analysis. All had MAF <0.01 in a non-founder population; additionally, variants representing haplotype associations or large genomic rearrangements were excluded. Estimates were derived for the two genes combined, with the justification that they exhibit broadly similar penetrance and phenotype, and there would be greater confidence in estimates based on the larger sample size for the combined dataset. Reference set variants were assigned to a frequency bin based on the maximum allele frequency observed in a non-founder sub-population (Non-Finnish European, African, Latino, East Asian, South Asian), from gnomAD Version 2.1.1 (non-cancer) accessed 2020-07-20. The dataset used for analysis is provided in Supplementary Table 3, and the details of LR estimation shown in Supplementary Table 4. LR estimates were correlated with ACMG code strength as per Tavtigian et al (Tavtigian et al., 2018).

An LR of 2.88 towards pathogenicity was estimated for absence of a variant in gnomAD, indicating PM2_Supporting as the strength for this evidence type. In addition, the LR estimation of other frequency bins was used to determine cut-offs

for BA1 (maximum allele frequency >0.001) and BS1 (>0.0001 to 0.001). In addition, analysis indicated that maximum allele frequency from >0.00002 to 0.0001 could conservatively be used to assign supporting evidence against pathogenicity (BS1_Supporting).

Variants under study were assigned a relevant ACMG-based frequency code based on the maximum allele frequency in a non-founder sub-population (described as above).

Bioinformatic-based codes

With respect to bioinformatic codes applied for potential spliceogenic variants, MaxEntScan (Yeo & Burge, 2004) scores in relation to native donor, native acceptor and cryptic site usage were reviewed to assign splicing-related bioinformatic codes (see Supplementary Table 1 for descriptions). These included review of MaxEntScan-based categories for native donor/acceptor site loss and donor gain following cut-point recommendations of Shamsani *et al.* (Shamsani et al., 2019), and additional consideration of MaxEntScan predictions of acceptor gain. The recommendations of Tayoun et al. (Abou Tayoun et al., 2018) were considered to determine codes applicable for variants directly impacting the donor and acceptor sites. Exon 3 donor site changes are predicted to abrogate the site and lead to an in-frame event that deletes amino acids 23-105, which includes most of the PALB2 interaction domain, originally conservatively defined as amino acids 10-40 (Xia et al., 2006). Although this is an in-frame deletion of a single exon, it was considered appropriate to upgrade PVS1_Strong to PVS1 for donor site changes since variants leading to complete *BRCA2* Δ E3 have demonstrated clinical characteristics

consistent with pathogenicity e.g., the LR in favor of pathogenicity based on segregation data for pathogenic control variant c.156_157insAlu was 6.41×10^{16} (Caputo et al., 2018). PVS1_Supporting was applied to single nucleotide substitution variants at the acceptor site, since the predicted effect was acceptor site abrogation and use of a nearby cryptic site to result in an aberrant transcript encoding a protein lacking two amino acids; the supporting code was assigned since the two amino acid deletion lies within the BRCA2-PALB2 interaction domain, and is bioinformatically predicted to impact protein function using BayesDel (see below).

Bioinformatic predictions (ESEfinder, RESCUE-ESE) for potential changes to Exonic Splice Enhancer or Silencer motifs (ESEs, ESSs) were recorded for comparison to splicing assay results, but not used to assign bioinformatic code. Similarly, variants were additionally reviewed for splicing-related predictions using the SpliceAI tool (Jaganathan et al., 2019), <https://spliceailookup.broadinstitute.org>, with the following parameters for each setting: genome version hg38, score type raw, max distance: 10000nt, Illumina's pre-computed scores yes, transcript NM_000059.4. Based on an analysis of previously published experimental and prediction data (Valenzuela-Palomo et al., 2022), SpliceAI predicted probabilities were assigned using a "two score" approach, whereby observation of two different scores >20% were considered predictive of leading to a splicing aberration. Namely, predicted exon 3 donor loss + exon 3 acceptor loss indicate predicted exon 3 skipping, predicted exon 3 donor loss + exon 3 (or intron 4) donor gain indicate predicted shorter (or longer) exon 3, predicted exon 3 donor loss + exon 4 acceptor

loss indicates predicted intron retention, etc. Conservatively, the lower of the two scores used to assign a given predicted splicing event was then used as the probability to lead to that predicted event. MES and SpliceAI predictions for consensus acceptor site variants are shown graphically in Supplementary Figure 2.

We used a combination of approaches to determine appropriate weights for bioinformatic codes for missense and in-frame indel variants. Substitution variants predicted (or shown) to alter splicing were excluded from datasets used for calibration. We first used heterogeneity analysis to determine the proportion of pathogenic variants considering location of these types of variants with respect to (likely) clinical important domains, and also *in silico* predicted impact of the alteration at the protein level. Previous heterogeneity analyses (Easton et al., 2007; Li et al., 2020; Tavtigian et al., 2008) have shown convincingly that missense variation *in toto* does not contribute much to *BRCA1/2* related disease, and further that there is strong evidence against pathogenicity for missense variants outside of a key functional domain. For the purpose of missense variant calibration, key functional domains were previously defined as those which contain individual missense variants previously determined to be pathogenic using clinical data. We conducted heterogeneity analysis as described recently (Li et al., 2020), using the exact same dataset, with the following alterations to the study design. In this analysis, we redefined the boundaries for known clinically important functional domains, added the *BRCA1* coiled-coiled domain as a potential clinically important domain (based on observation of Fanconi anemia like abnormalities in mice

homozygote for a coiled-coiled domain deletion (Nacson et al., 2020), and extended the calibration to compare results for BayesDel (<http://fengbj-laboratory.org/BayesDel/BayesDel.html>) to the A-GVGD prediction tool (<http://agvgd.hci.utah.edu/>) assessed in previous heterogeneity analyses. While both tools predict variant impact on protein function via missense substitutions, BayesDel has capacity to additionally predict impact of in-frame indels. Briefly, we estimated the proportion of pathogenic variants in the dataset that are likely to be clinically significant as a function of bioinformatically predicted classifications, and variant location in a domain (see Supplementary Table 5 for details, including definitions of domains). Results indicated that there is convincing evidence against pathogenicity for missense/in-frame protein alterations outside of a known clinically important domain: only 1% of variants in this category were estimated to be pathogenic (Supplementary Table 5). Stratification using BayesDel score identified few variants with predicted impact on protein function (n=42, 2.7% of this subgroup, with only 7% of such variants predicted to be pathogenic based on clinical presentation). Further, for missense variants *within* the recognized clinically important functional domains, BayesDel had improved capacity to identify pathogenic variants over A-GVGD. For BayesDel Score ≥ 0.30 , 83% of variants were estimated to be pathogenic, compared to 74% for A-GVGD. Note, we did not use the results from this analysis to formally derive LRs for ACMG code strength assignment, due to expectation of bias in the LR estimates. This clinically-generated dataset was not annotated for missense variants previously determined to be benign on the basis of frequency or other information (since these are not reported

clinically), and thus the overall proportion of variants annotated as (likely) pathogenic or VUS is likely higher than would be expected for a dataset with complete annotation of missense variation.

We used the following approach to define LRs for pathogenicity. We reviewed the evidence for pathogenicity for *BRCA1* and *BRCA2* missense substitution variants by domain from a recent large-scale case-control study, including 60,466 breast cancer cases and 53,461 controls (Breast Cancer Association et al., 2021). The results provided no evidence that missense variants located outside a domain were overall associated with increased risk, with risk estimates as follows: *BRCA1* OR 1.02 (0.94-1.10), *BRCA2* OR 0.97 (0.92-1.03). Given that case-control data may be used to provide strong evidence in favor of pathogenicity (ACMG/AMP code PS4), it seems logical to assert that these case-control findings provide strong evidence against pathogenicity for missense variants located outside of a protein domain. Indeed, this assertion is consistent with the results of an analysis of ClinGen submitter classifications for *BRCA1* and *BRCA2* variants according to protein domain (Dines et al., 2020), which provided evidence that variants in “coldspots” could be assigned a strong benign category based on their location alone.

For *BRCA1* and *BRCA2* missense substitution variants within a domain, we then estimated LRs for missense variants according to BayesDel score category, using functional impact as a surrogate for variant pathogenicity (Supplementary Table 6). Functional impact was assigned based on the aggregated results from nine studies (Supplementary Table 7). As above, variants known or predicted to alter splicing

were excluded, as were variants with conflicting results between studies, since from our observation these largely reflect experimental design issues that fail to capture mRNA aberrations. LRs were estimated separately for variants with no functional impact, partial impact, or complete impact. BayesDel score was not significantly predictive of partial impact on function. BayesDel score <0.3 was predictive of no impact on function, with derived LRs consistent with a Supporting Benign code. BayesDel score ≥ 0.3 was predictive of complete impact on function, with derived LRs consistent with a Moderate Pathogenic code. Considering also results from Supplementary Table 5, BayesDel categories <0.3 and ≥ 0.3 were conservatively considered as supporting evidence against (score <0.3) or towards (≥ 0.3) pathogenicity for missense variants within a domain.

None of the analyses denoted above estimated values for synonymous variants. However, the assumption is that silent variants (with no predicted impact on splicing) outside of a clinically important domain can be assigned the same Benign code strength as that for any missense alteration (with no predicted impact on splicing) outside of a clinically important domain i.e. BP7_Strong. Following the same logic, silent variants (with no predicted impact on splicing) located within a domain could be assigned the same evidence strength as missense variants with low predicted impact on function via effect on protein (BayesDel score <0.30). Further, since intronic variants outside of the consensus donor/acceptor motif (with no predicted impact on splicing) are commonly viewed as akin to synonymous variants, we suggest conservatively the assignment of a BP7_Moderate code, to

recognize limitations of bioinformatic tools in prediction of pseudoexonization (Canson et al., 2020).

We thus determined the following conservative recommendations for variants outside of the consensus sites, based on predictions using MaxEntScan for splicing, and BayesDel for missense/in-frame alterations:

- **PP3** for silent, intronic or missense **variation predicted to alter splicing** (for exonic variants, irrespective of location in a domain)
- **PP3** for **missense variation within a key domain**, and predicted effect via missense alteration (BayesDel scores ≥ 0.30), having excluded possible impact on splicing.
- **BP4** for **missense variation within a key domain**, and low predicted effect via missense alteration (BayesDel scores < 0.30), having excluded possible impact on splicing.
- **BP1_Strong** for **missense variation outside of a key domain**, having excluded possible impact on splicing.
- **BP7_Strong** for **synonymous variants located outside of a key domain**, having excluded possible impact on splicing.
- **BP7** for **synonymous variants located inside a key domain**, having excluded possible impact on splicing. Also apply for **intronic variants located within donor and acceptor motifs** (up to and including +8, -12 into the intron), and no predicted impact on splicing.

- **BP7_Moderate.** Apply for **intronic variants located outside of donor/acceptor motifs** (+9 or more, -13 or more), and no predicted impact on splicing.

The codes applied for each variant are noted in Supplementary Table 1. For this analysis restricted to *BRCA2* exon 3 variants only, key domain referred to the PALB2 interaction domain captured within exon 3, designated conservatively as amino acids 23-40 (Oliver et al., 2009; Xia et al., 2006). Predictions for BayesDel were annotated from Version 1 database (build date 2017-08-24) excluding allele frequency. For missense variants, BayesDel used a combination of individual deleteriousness scores including FATHMM, GERP++, LRT, Mutation Assessor, Mutation Taster, Polyphen2_HDIV, Polyphen2_HVAR, PROVEAN, SIFT, SiPhy_29way, VEST3, fitCons, fathmm-MKL coding, phastCons 100way, phastCons 20way, phyloP 100way, and phyloP 20way. For in-frame indels, BayesDel score is calculated using PROVEAN. An overview of the process for assigning bioinformatic codes is described in the results section.

Functional-based codes:

Splicing data from this study and several publications were summarized to assess the clinical relevance of the result, accounting for assay method or RNA source. Intronic and synonymous variants with only $\Delta E3$ observed, at a level similar to or below that seen for known benign variant *BRCA2* c.68-7T>A, were automatically designated to be of no clinical importance and code BS3 was assigned. We also reviewed the clinical data supporting variant assertions for variants assayed by Tubeuf *et al.* using mESC (Tubeuf et al., 2020), and *conservatively* extended BS3

code assignment to variants with up to 30% per-allele exon exclusion, either directly measured (mESC functional assay), or inferred (heterozygous samples). This conservative assignment was based on data for the common synonymous variant c.231T>G (maximum MAF > 1%), reported to demonstrate 30% Δ E3 in a minigene assay, and 32-40% Δ E3 and complementation of the null phenotype in a mESC assay (Tubeuf et al., 2020). Note, although results from the same study suggested a higher level of Δ E3 in LCL-derived mRNA (55%, ~85% inferred per-allele Δ E3 for the G allele), there was evidence for variability across repeats for this sample (Tubeuf et al., 2020), and review of experimental design and data for control variants c.68-7T>A revealed potential for preferential amplification of shorter Δ E3 fragments.

PS3 via effect on mRNA was assigned for near-complete Δ E3, defined as $\geq 90\%$ Δ E3, based on previous observations for mini-gene results for variants with convincing clinical data supporting pathogenicity (Caputo et al, 2018). In instances where transcripts encoding small in-frame deletions were identified, no functional code was assigned unless results were available from the mESC assay that captured both mRNA and protein effects (see above). Based on calibrations against assay results reported in Mesman *et al.* (Mesman et al., 2019) for variants classified as (likely) pathogenic or (likely) benign against a model of high cancer risk (Parsons et al., 2019) (Supplementary Tables 8 and 9), PS3 was assigned for variants which showed poor complementation in the mESC assay (<20% viability), and BS3 for variants with complementation and HDR activity >50%. In the absence of previous calibration data for variants with reduced complementation based on clone count

(20-50% viability), combined complementation and HDR were reviewed for the single variant with reduced complementation; given that HDR activity of 51% for c.316+6T>G variant falls at that bottom of the range for (likely) benign variants, the result was considered unclear, and no functional code was assigned. We also compared our findings for mESC assays to those of Tubeuf *et al.* (Tubeuf *et al.*, 2020) for overlapping variants, summarized in Supplementary Table 10.

In summary, conservative application of functional-based codes was as follows:

- **BS3** for intronic and synonymous variants with mRNA results detecting only $\Delta E3$ at a level qualitatively determined to be similar to or below that seen for known benign variant *BRCA2* c.68-7T>A, or per-allele $\Delta E3$ measured as up to 30%.
- **BS3** for variants (intronic, synonymous, missense) with complementation and HDR activity >50%, and no conflicting mESC results in the literature.
- **PS3** for intronic and synonymous variants with near-complete $\Delta E3$ ($\geq 90\%$ exon skipping).
- **PS3** for variants (intronic, synonymous, missense) which showed poor complementation in the mESC assay (<20% viability), and no conflicting mESC results in the literature.

For a small subset of predicted missense variants with no clinically relevant impact on splicing, results from functional studies were drawn from previous publications (Ikegami *et al.*, 2020; Mesman *et al.*, 2019), and assigned BS3 if reported to have no impact on function, or PS3 if reported to have impact on function.

Clinical data codes:

Bayes scores for segregation were derived as described previously (Thompson et al., 2003). Additional Bayes scores for segregation, derived using the same approach, were taken from previous publications (Caputo et al., 2018; Caputo et al., 2021; Easton et al., 2007; Goldgar et al., 2004). In addition, the Bayes segregation score for c.93G>T p.(Trp31Cys) derived using a very similar method (Mohammadi et al., 2009), was extracted from Biswas *et al.* (Biswas et al., 2012). Likelihood ratios (LRs) for breast tumor pathology were applied according to Spurdle *et al.* (Spurdle et al., 2014). LRs previously derived based on co-occurrence data (Easton et al., 2007) and personal and family history presentation (Caputo et al., 2021; Easton et al., 2007; Li et al., 2020) were also incorporated into the analysis. Segregation, pathology, co-occurrence and personal/family history LRs were combined by multiplication to derive a combined odds towards causality (Goldgar et al., 2008). The combined clinical data was then assigned the relevant code strength based on “odds of pathogenicity categories” arising from a Bayesian re-analysis of the ACMG/AMP variant classification guidelines (Tavtigian et al., 2018).

LR ranges for categories are summarised below:

- **Strong:** Benign <0.05 to 0.00285; Pathogenic >18.70 to 350
- **Moderate:** Benign <0.23 to 0.05; Pathogenic >4.30 to 18.70
- **Supporting:** Benign <0.48 to 0.23; Pathogenic >2.08 to 4.30
- **No evidence:** 0.48 to 2.08

The sources of information compiled for classification are detailed in Supplementary Table 1, with provenance of data collected as part of this study shown in Supplementary Table 11.

Additional codes:

The ACMG/AMP code PS1 is strong pathogenic evidence defined as “same amino acid change as a previously established pathogenic variant regardless of nucleotide change”. This description was applied in the context of a variant outside of the consensus splice site with a similar predicted impact on mRNA splicing as another variant at that nucleotide position, for which the classification is determined to be pathogenic from **clinical** and other data (PS1(Splicing)). The code was also applied conservatively at supporting level for variants already assigned a PVS1 code due to location at the consensus dinucleotide, and for which there was another variant located at the same consensus dinucleotide that was classified as pathogenic from **clinical** and other data (PS1_Supporting (Splicing)); this conservative approach prevents overweighting of a consensus site variant compared to the “original” pathogenic consensus site variant. The PS1 code was not applied for missense variants in this study, since there were no relevant variants for which it was applicable. We did not consider application of PM5, a missense substitution (with no predicted/known effect on mRNA splicing), located at a residue for which a pathogenic missense variant is known to occur, following the rationale that this code is more effectively captured by our clinically calibrated bioinformatic code combining domain and predicted missense effect. We also did not assign PM1, since our application of bioinformatic scores already accounted for domain.

Combining Criteria to derive final class:

We first derived class using the original ACMG/AMP code combinations (Richards et al., 2015), following recommendations for minor changes in combinations arising from the Bayesian framework analysis of Tavigian et al (Tavigian et al., 2018).

Then for comparison, codes were combined following the point system approach recently proposed to simplify scoring and class assignment (Tavigian et al., 2020). Point values assigned for the different code strengths were as recommended in the original publication: Indeterminate=0; Supporting=1, Moderate=2, Strong=4 and Very Strong=8 for Pathogenic codes; negative values for Benign codes of same strength. Point ranges to assign class followed the conservative recommendations in the original publication: Benign ≤ -7 , Likely Benign -6 to -2, Uncertain -1 to 5, Likely Pathogenic 6-9, Pathogenic ≥ 10 .

Results

A comprehensive summary of splicing, functional and clinical data, encapsulating data generated as part of this study and that from previous publications, is shown in Supplementary Table 1. Summary mRNA and/or functional data generated as part of this study (WT reference, four controls and another 32 variants), together with a final classification based on combine evidence, is shown in Table 1. The sections below detail findings from analyses conducted as part of this study.

mRNA transcript analysis using minigenes and patient samples

Details of mRNA results shown in Supplementary Figure 3 (minigene results) and Supplementary Figure 4 (patient mRNA results), and findings are summarized in

Table 1. Excluding control variants, minigene assays were performed for 21 unique variants, and splicing assays on patient mRNA were performed across multiple labs for 14 unique variants. Considering results from either approach, assay results for a total of 15 variants indicated that $\Delta E3$ was at levels considered clinically unimportant (not detectable, at low levels comparable to wildtype, or similar to that of benign control c.68-7T>A), and there was no other impact on mRNA splicing.

Using qualitative comparisons to control variants, minigene or patient mRNA analysis showed three variants to exhibit $\Delta E3$ at levels greater than that of benign control c.68-7T>A: c.68-3T>G, c.277_317-726delinsCCAT, and c.316+1G>T. Variant c.68-3T>G, predicted by MaxEntScan to inactivate the acceptor site (6.10 \rightarrow 0), showed increased $\Delta E3$ by minigene analysis. Complex variant c.277_317-726delinsCCAT deletes the donor site sequence, and analysis of mRNA from stabilized blood is concordant with previous analysis by Nordling *et al.* (Nordling *et al.*, 1998) that the variant induces a high level of $\Delta E3$. Donor site variant c.316+1G>T, previously shown to lead to complete $\Delta E3$ by minigene assays (Caputo *et al.*, 2018), was confirmed to show high levels of $\Delta E3$ in mRNA from stabilized blood.

All variant substitutions impacting the native acceptor AG dinucleotide were predicted to abolish the acceptor site, and also to strongly increase the score for a cryptic splice site at position c.74 (2.17 \rightarrow 7.77) (Supplementary Figure 2). Minigene analysis showed evidence of slightly increased $\Delta E3$ (for c.68-2A>G and c.68-1G>A), and use of the c.74 cryptic splice site as a major event; the latter major event was confirmed by sequencing of patient mRNA for c.68-2A>G

(Supplementary Figure S3b and S4b). The mRNA transcript arising from use of the cryptic splice site $\Delta(E3p6)$ encodes an in-frame deletion of two amino acids, p.Asp23_Leu24del. Minigene assays supported use of c.74 for five additional single nucleotide substitutions at the splice site, with a slight increase in $\Delta E3$ observed for c.68-1G>A (Supplementary Figure S3b, Table 1).

Variant c.72_85delinsTTTAAATAGAT was not predicted to alter the WT acceptor (MaxEnt score 6.10), but a new predicted acceptor sequence (MaxEnt score 3.33) is introduced in the inserted sequence. Splice assays for c.72_85delinsTTTAAATAGAT using LCL and PAXgene® mRNA provided evidence for usage of the *de novo* acceptor site in addition to $\Delta E3$ levels in the broad range (or higher depending on sample type) observed for benign control c.68-7T>A (Figure 1, Supplementary Figure S4a). The resulting mRNA transcript encodes a protein with deletion of six amino acids and insertion of five new amino acids p.(Leu24_Leu29delinsPheLeuAsnArgPhe).

$\Delta E3$ level quantification by dPCR in patient-derived RNA samples

dPCR on 16 patient-derived RNA samples was performed to more accurately quantify exon 3 exclusion. In particular, this was necessary to compare $\Delta E3$ level observed for individual variants to that observed for known pathogenic or benign control variants known to lead to $\Delta E3$. Depending on sample type (directly stabilized blood, short term cultures, or LCLs), dPCR analysis showed absolute exclusion levels of 5.7%-14.5% for the benign “partial” skipping control c.68-7T>A sample, while absolute exclusion levels for the complete $\Delta E3$ control variants ranged from 44.9% (c.316+5G>A; blood) to 52.3% (c.156_157insAlu; LCL) (Figure 1A). The

inferred per-allele $\Delta E3$ levels for the c.68-7A allele (Figure 1B, Table 1) were 8.7% (blood), 14.7% (lymphocyte) and 25.2% (LCLs), with per-allele exclusion for “complete $\Delta E3$ ” variant controls ranging from 87.0% (c.316+5G>A; blood) to 100.0% (c.156_157insAlu; LCL).

To investigate the impact of previously reported naturally occurring multi-exon skipping transcripts, we analyzed $\Delta E3-E4$ and $\Delta E3-E7$ for full exon 3 skipping variants c.316+1G>T and c.316+5G>A, and benign control c.68-7T>A. Very low exclusion levels (i.e., lower than 3% in all cases) for the multi-exon skipping transcripts were observed across multiple tissue types (Supplementary Figure 5).

RNA sequencing analysis of patient-derived RNA samples

RNAseq analysis was performed in c.68-3T>G (N=2), c.68-2A>G (N=5), and c.68-1G>A (N=1) carriers, as well as in control samples (N=2) (Supplementary Figure 6). In c.68-3 T>G carriers, $\Delta E3$ (20.4% of reads; range 19.0-21.9%) and $\nabla E3p2$ (16.7%; range 14.5-19.0%) were the predominant aberrant transcripts. In c.68-2A>G and c.68-1G>A carriers, the predominant aberrant transcripts were $\Delta E3p6$ (28.9%; 26.0-31.1% and 36.8%, respectively) and $\Delta E3$ (8.2%; 6.6%-10.2% and 7.9%, respectively). Control samples expressed $\Delta E3$ at low levels (2.7%; 2.4-3.0%). Table 1 and Figure 2 show the corresponding inferred per-allele expression levels. RNAseq detected other transcripts both in controls and variant carriers (including $\Delta E3-E4$), although at very low levels (i.e. less than 3%).

Inferred clinical relevance of splicing patterns

For the interpretation of variants, we reasoned that the effect on mRNA splicing will not have a significant clinical impact for any variant with a per-allele $\Delta E3$ level similar or lower than observed for c.68-7T>A, if no other alternative splicing events are detected. Taking into account mRNA sample source, this deduction could be applied for seven variants in the study: c.68-7delT, c.68-7dupT, c.116C>T, c.125A>G, c.198A>G, c.223G>C and c.280C>T (Table 1). The combination of minigene data (Supplementary Figure S3c), patient assay results (Supplementary Figure S4i) and dPCR inferred per-allele $\Delta E3$ level (17.1%, Figure 1B) for c.91T>C, suggested at best a modest increase in $\Delta E3$ for this variant. $\Delta E3$ was slightly increased above that of c.68-7T>A for variant c.68-3T>G (29.7%)(Figure 1B, Table 1), with per-allele $\Delta E3$ level using RNA-sequencing methodology of 38.1% (Figure 2).

The clinical interpretation of splicing results was less clear for the following variants, due to the somewhat increased levels of $\Delta E3$ relative to WT controls, presence of additional aberrant (in-frame or other) transcripts, and/or ability of the variant-induced mRNA transcript to encode a protein with an in-frame alteration in amino acid sequence. Variants c.68-2A>G and complex deletion-insertion variant c.72_85delinsTTTAAATAGAT displayed a more complex mRNA transcript pattern, including different aberrant in-frame transcripts (Supplementary Figure S4a-b) in combination with increased $\Delta E3$. Inferred per-allele $\Delta E3$ levels for c.68-2A>G were 19.4% (blood), and for c.72_85delinsTTTAAATAGAT were 20.8% (blood) and

49.2% (LCL). Results for c.68-2A>G were similar by RNA-sequencing, with average 57.9% inferred per-allele expression of a transcript encoding p.Asp23_Leu24del, in addition to average 13.6% inferred per-allele expression of Δ E3 (Figure 2). Variant c.277_317-726delinsCCAT displayed a greater proportion of Δ E3, with dPCR per-allele Δ E3 level of 54.6% in patient mRNA from stabilized blood (Figure 1).

Variant c.316+1G>T displayed extensive Δ E3 relative to controls (inferred per-allele 79% in patient mRNA from stabilized blood, >100% in mRNA from short term lymphocyte culture), consistent with a severe impact on the exon 3 donor site.

Functional characterization of *BRCA2* exon 3 region variants using a mouse embryonic stem cell-based assay

To directly assess the functional impact of variant-induced Δ E3 and/or effect on protein via change in amino acid sequence, we utilized a mouse embryonic stem cell-based (mESC) assay validated against known pathogenic and benign missense variants (see methods). Wild-type *hBRCA2*, benign control variants c.68-7T>A and c.231T>G, pathogenic control variant c.316+5G>C, and another 18 *BRCA2* gene variants were transfected into hemizygous mESC.

Analysis of Δ E3 level in mESC-derived RNA samples

Variants c.316+1G>T and c.316+5G>C showed near complete exon 3 skipping (99.7% and 99.1% Δ E3, respectively) in mESC-derived mRNA (Supplementary Figure S7). Variants c.316+6T>A and c.316+6T>G displayed severely increased Δ E3 transcript levels (80%), while c.316+6T>C displayed a more moderate level of

$\Delta E3$ (56%). For synonymous variants c.102A>G and c.231T>G, $\Delta E3$ levels were 35% and 20%, respectively. The $\Delta E3$ level for c.68-2A>G (12.8%) and c.68-3T>G (9.9%) was comparable to the $\Delta E3$ level observed for benign variant c.68-7T>A (13.3%). For c.72_85delinsTTTAAATAGAT $\Delta E3$ level was approximately double (23.5%) that observed for c.68-7T>A. For the other variants, $\Delta E3$ was either not detected, or detected as a minor event at levels below that observed for c.68-7T>A. Capillary electrophoresis of RNA for variant c.68-2A>G (Supplementary Figure S8) confirmed expression of the transcript lacking 6 bases ($\Delta E3p6$) in addition to $\Delta E3$. As summarized in Supplementary Table 10, overall trends in observed mESC splice patterns from assays in this study (Table 1), were in line with those previously published (Tubeuf et al., 2020), considering differences in experimental design that have previously been shown to overestimate levels of the smaller $\Delta E3$ products (Colombo et al 2018). As expected, the absolute per-allele $\Delta E3$ level from ddPCR analysis (this study) was consistently lower than that measured using semi-quantitative RT-PCR (Tubeuf et al 2020), and differences were more marked for samples/variants with lower $\Delta E3$ (WT control, c.102A>G, c.231T>G). Despite this, the bioinformatically predicted probability of exon exclusion for the three variants at the +6 position appeared to correlate with within-study relative levels of $\Delta E3$ expression.

The functional impact of BRCA2 exon 3 variants

Complementation phenotype, the ability of variants to rescue the lethal cell phenotype upon *mBrca2* loss, is shown in Supplementary Figure S9. Confirmation of protein expression is shown in Supplementary Figure S10. Poor

complementation, indicative of loss of protein function, was observed for the pathogenic control c.316+5G>C, variant c.316+1G>T known to lead to (near) complete $\Delta E3$, and another five variants (c.72_85delinsTTTAAATAGAT, c.91T>C, c.91T>G, c.93G>C; c.93G>T). Variant c.316+6T>G displayed reduced complementation (20-50% viability), and all other variants revealed a good complementation capacity (>50% viability relative to wildtype).

The 14 variants (including benign control variant c.68-7T>A) with reduced or good complementation (Supplementary Figure S9), were assessed for HDR capacity (Figure 3). All variants demonstrated HDR activity above 50%, in the range previously observed for variants classified as (likely) benign using multifactorial likelihood analysis approaches. Notably, variant c.316+6T>G with reduced complementation displayed 51% HDR, just above the lower boundary previously defined for BRCA2 missense variants classified as (likely) benign using multifactorial likelihood approaches (Mesman et al., 2019).

As shown in Supplementary Table 10, mESC complementation and secondary analysis results were also compared to those reported for overlapping variants assayed using related methodology by Tubeuf et al (2020). This revealed apparent differences in results for the c.316+6T>A and c.316+6T>G variants, complicated by differences in viability thresholds used to assign complementation category and differences in secondary analysis approaches. Given that the level of $\Delta E3$ (as measured by either study) fell outside the range set for assigning PS3 or BS3, no

functional code was assigned for these two variants. Results for variant c.316+6T>C were consistent across the two studies (good complementation).

Classification of variants using a gene-specific adaptation of the ACMG/AMP criteria

This study included analysis of four control variants classified with respect to pathogenicity (benign controls c.68-7T>A, c.231T>G; pathogenic controls c.156_157insAlu, c.316+5G>C), complete $\Delta E3$ experimental control c.316+5G>T, and another 84 variants from the *BRCA2* exon 3 region. Clinical, splicing and functional data collected for this study, or derived from previous publications, were used to assign a classification following a gene-specific adaptation of the ACMG/AMP criteria (see methods for details; of necessity, the PVS1 codes derived are for exon 3 donor and acceptor only, and applicable at the level of exon). Figure 4 provides an overview of the application of codes relating to variant position and bioinformatic prediction of effect, and subsequent interpretation and code application relating to mRNA and functional data.

Specifically, classification categories were assigned using the point-based ACMG/AMP system, allowing the application of additional LR-based benign code strengths for clinical data, and a greater range of options to combine benign and pathogenic data points compared to the code-combinations originally proposed (Richards et al., 2015; Tavgigian et al., 2020). The breakdown of variant classifications using the points-based approach was as follows: 31 Benign, 32 Likely Benign, 16 Uncertain, two Likely Pathogenic and four Pathogenic (Supplementary Table 1). For 1 Likely Pathogenic, 11 Benign and 26 Likely Benign points-based

variant classifications, classifications were at a lower confidence level or uncertain using the original code combinations. Of the four variants classified as Pathogenic, one was the complete skipping experimental control c.316+5G>A, another two also led to complete exon 3 skipping (c.277_317-726delinsCCAT, c.316+1G>T), and the other was the complex deletion-insertion variant c.72_85delinsTTTAAATAGAT which led to an in-frame change in protein sequence predicted bioinformatically to impact function. The Likely Pathogenic classifications for variants c.91T>C p.(Trp31Arg) and c.92G>C p.(Trp31Ser) were driven by direct and/or clinical evidence of functional impact via the missense change, since there was no evidence for altered splicing for either variant.

Of interest is that the exon 3 acceptor site variants were assigned a low bioinformatic code of PVS1_Supporting due to MaxEntScan-predicted use of a cryptic acceptor site resulting in an aberrant transcript encoding a two amino acid deletion (Table 1). We note that the more recently developed SpliceAI tool also predicted high probability of using the cryptic splice site (>95%) for all six single nucleotide substitutions (Supplementary Figure 2). The assigned conservative annotation for this acceptor site was justified by observations from splicing and functional assay results. All six acceptor site variants were confirmed to induce this in-frame aberrant transcript lacking the six nucleotides in minigene assays, with modest level of $\Delta E3$ also observed for some variants. Similarly, RNA-sequencing analysis of patient material showed a ~3-fold enrichment of transcripts resulting from cryptic splice site usage compared to those due to $\Delta E3$ (Supplementary Figure

S6c). For c.68-2A>G, both $\Delta E3$ and the 6bp deletion transcript were detected in analysis of mESC RNA (Supplementary Figure S8). Variant c.68-2A>G displayed good complementation and HDR capacity 70%; this finding, together with available clinical evidence against pathogenicity was sufficient to assign a Likely Benign classification. The remaining 5 possible acceptor site variants are currently considered Uncertain, largely due to lack of information.

Due to inconsistencies in mESC complementation results between this study and that of Tubeuf *et al.* (Tubeuf et al., 2020) for the c.316+6T>A and c.316+6T>G variants (despite roughly concordant levels of $\Delta E3$, accounting for differences in mRNA assay design), functional assay codes were not applied for them. Between-study mESC results were consistent for c.316+6T>C. Considering all applicable codes, c.316+6T>A and c.316+6T>G remained VUS, while c.316+6T>C was classified as Likely Benign.

Discussion

In this study, we used a variety of approaches to calibrate individual evidence types and justify code weights tailored for classification of so-called high-risk pathogenic variants in BRCA1 or BRCA2. We then assessed the utility of these calibrated codes for classification of variants in/near *BRCA2* exon 3, selected as an exemplar for highlighting challenges around interpreting the clinical impact of in-frame deletions (at genomic or mRNA level) that target a known clinically relevant functional domains. Using a point-based (Tavtigian et al., 2020) gene-specific

adaptation of the ACMG/AMP criteria, and laboratory assay and clinical data generated from our own work or by previous studies, classification was assigned for 69/85 (81%) of variants in the *BRCA2* exon 3 region (Supplementary Table 1). This practical application of the point-based method demonstrated that it was especially beneficial for classification of variants in the benign direction, increasing a class assignment from 49% (42/85) to 81% (69/85). First, the conceptual advantage of the point system is that codes of any strength (for or against pathogenicity) can be combined arithmetically - with a wider range of options for code combinations in the same direction. Notably, it allows the application of points equivalent to benign moderate, a code that does not exist in the baseline ACMG/AMP system. Further, it simplifies the process for code combinations where evidence may be in the opposing direction, and promotes flexibility to apply additional evidence types in both directions, assuming there is justification for the code strength applied e.g. from clinical calibration. In addition, our study highlights a number of other issues for consideration, as elaborated below.

Annotation of splicing predictions – value and challenges

Our analysis also highlights the importance of careful annotation of predictions for splice site variants, as recommended by Tayoun *et al.* (Abou Tayoun et al., 2018). All exon 3 splice site variants located at the $\pm 1/2$ positions might reasonably have been annotated as PVS1 due to expectation of $\Delta E3$ and in-frame deletion of a clinically important functional domain. However, the cryptic site prediction for the acceptor site variants indicated the possibility of an altered transcript encoding a

protein with a two amino acid deletion (p.Asp23_Leu24del), for which there was no existing laboratory evidence for impact on function at the time of our study. Our combined splicing assays showed that all acceptor site variants produced the $\Delta E3p6$ transcript, with modest expression of the $\Delta E3$ for the c.68-2A>G and c.68-1G>A substitutions. Indeed, a recent study (Nix et al., 2021) has highlighted c.68-2A>G as a variant of uncertain clinical significance, on the basis of evidence against pathogenicity derived from an in-house family history weighting algorithm, and detection of the in-frame aberrant transcript in 39% of the total transcript pool for blood-derived mRNA (quantified using a dilution-based method). It is notable that mESC analysis results from our study, which consider impact via mRNA splicing and encoded protein simultaneously, show that the acceptor site variant c.68-2A>G permits complementation, with HDR characteristics of surviving cells consistent with variants categorized as (likely) benign using multifactorial likelihood analysis methodology. Further, the combined clinical data for this variant provided moderate evidence against pathogenicity. Together these findings indicate that the c.68-2A>G variant does not exhibit the functional and clinical features of so-called “high-risk” *BRCA2* variants. We acknowledge that the calibrated evidence types applied here may not reliably detect variants with reduced penetrance relative to the average *BRCA2* premature termination codon variant; alternative analyses, such as large-scale case-control analyses, would be required to assess if c.68-2A>G (and other acceptor site variants) may be associated with low-moderate risk of cancer. We note that this variant is reported 2 times as Likely Pathogenic in Clinvar, based

largely on location at a splice site and expectation to cause aberrant splicing and lead to loss of function.

$\Delta E3$ upregulation in at least one assay (>10%) was observed for 11 variants not predicted to affect splicing by our initial MaxEntScan bioinformatic analysis (focused on donor/acceptor loss or donor gain: control variant c.231T>G; c.72_85delinsTTTAAATAGAT; c.91T>C; c.91T>G; c.93G>C; c.93G>T; c.100G>A; c.102A>G; c.316+6T>A; c.316+6T>G; c.316+6T>C. We also reviewed prediction against the SpliceAI tool (Jaganathan et al., 2019) which is becoming more commonly used in the research and clinical setting. Of these, only two were predicted to alter splicing by SpliceAI at a probability threshold of 20% or greater, using the two score approach described in the methods: variant c.316+6T>G with SpliceAI probability of 25% to lead to $\Delta E3$, and demonstrating 77% to 88% $\Delta E3$ across multiple assays; variant c.100G>A p.(Glu34Lys) with 20% probability to lead to $\Delta E3_{p45}$, and splicing assays showing variously 14%-57% $\Delta E3$, at higher levels than $\Delta E3_{p45}$ and additional transcripts. These observations suggest that it is appropriately conservative to apply only supporting level of evidence for splicing donor/acceptor loss/gain predictions for variants outside of the consensus site, in the absence of large-scale calibration efforts. Further, it is notable that the vast majority of variants were predicted to alter at least one ESE motif using ESEfinder or RESCUE-ESE (Supplementary Table 1), but showed no marked effect on splicing. It is possible that other ESE prediction tools may have better predictive

value (Canson et al., 2020), but such analysis was considered outside the scope of this study.

Using mRNA and functional assay data from multiple sources – benefits and challenges

One particularly challenging aspect of this study was interpreting mRNA and functional data generated using a variety of approaches, including use of different mRNA sources and functional assay designs. Moreover, mRNA results were not recorded consistently, with the two main sources of published data presenting findings as % full length relative to WT (Tubeuf et al., 2020), and % canonical and other transcripts in the total transcript pool for an individual (Fraile-Bethencourt et al., 2019). Further, a majority of previous results were generated using RT-PCR methods that can severely overestimate levels of the smaller $\Delta E3$ product; indeed data previously published for LCL-derived mRNA for variant c.68-7>A (Colombo et al 2018) reports $\Delta E3$ signal to be 33% using RT-PCR versus ~12% using ddPCR. To better compare minigene and mESC assay results measuring effect of a single allele, we calculated an inferred per-allele $\Delta E3$ level for variants assayed using mRNA analysis of patient material. We observed that the $\Delta E3$ level varied somewhat for different blood-related samples, with a tendency for higher $\Delta E3$ level in LCL samples than in other sample types. This was the case for both carrier and non-carrier samples, and the levels correlated across tissue type. For example, c.72_85delinsTTTAAATAGAT showed an inferred per-allele $\Delta E3$ level of 49.2% in LCL-derived mRNA versus 20.8% in mRNA from a PAXgene® sample. Since

mRNA analysis results were very reproducible across several technical replicates, and the PAXgene® and LCL samples assayed for the c.72_85delinsTTTAAATAGAT variant were from the same individual, results suggest different absolute level of $\Delta E3$ in different cell types. We thus utilized the $\Delta E3$ levels for known benign variant c.68-7T>A as a strategy to account for differences by sample type.

We also show the importance of using minigene assays, conventional mRNA analysis combined with Sanger sequencing, and RNA-sequencing to detect small changes in mature transcript. Notable examples were detection of the $\Delta E3p6$ transcript (encoding p.Asp23_Leu24del) for the exon 3 acceptor site variants, and detection of $\nabla E3p2$ for variant c.68-3T>G.

Our findings highlight the value of the mESC assay to provide data on both RNA splicing impact and overall functional consequence. While our results indicate similar mRNA transcript expression patterns in mESC and patient samples by dPCR quantitation of $\Delta E3$, the major advantage of this model was that it allowed analysis of the effect of intronic and exonic variants on mRNA splicing in a monoallelic manner. Such effects spanned in-frame exon skipping at various levels and “aberrant” in-frame protein coding events, and transcripts encoding a missense change, or a small in-frame deletion (as observed for c.68-2A>G), and variants that resulted in complex transcript profiles. Despite these advantages, we caution that functional assay methods in general have been calibrated against reference set variants classified using clinical and other features that define them as high-risk pathogenic or not. That is, we cannot exclude the possibility that some variants, in

particular those identified as presenting with conflicting results between studies and or other inconsistencies in presentation, may represent hypomorphs potentially associated with reduced (even modest) risk of cancer.

Possible future directions arising from laboratory findings

In addition to the important role of functional data in variant classification, the functional data have provided several interesting research questions to be addressed in future studies. Acceptor site variant c.68-2A>G resulted in modest $\Delta E3$ upregulation, and a transcript encoding p.Asp23_Leu24del. In the mESC assay the same transcripts were expressed, and the overall assay results indicated that the impact of the variant is inconsistent with high risk. This would suggest that amino acids 23 and 24 are not absolutely critical for the PALB2-binding function of this protein domain. Functional data from previous studies (Biswas et al., 2012; Ikegami et al., 2020), and our analysis suggest that p.Trp31 is a critical residue in this domain; c.91T>C (p.Trp31Arg), c.91T>G p.(Trp31Gly), c.93G>C p.(Trp31Cys) and c.93G>T p.(Trp31Cys) demonstrated no/poor complementation in the mESC assay. Indeed, mESC data is in agreement with structural analysis showing that p.Trp31 (but not Asp23 or Leu24) is critical for BRCA2-PALB2 interaction (Oliver et al., 2009), and clinical data reported by Caputo *et al.* (Caputo et al., 2021) indicating that c.92G>C p.(Trp31Ser) is associated with high risk of cancer.

Splicing and functional data was thoroughly reviewed to provide insight into the relationship between full-length *BRCA2* transcript expression and protein activity in combination with exon 3 skipping. We have demonstrated the importance of using

tissue-matched controls as reference (benign variants known to lead to increased $\Delta E3$, in addition to wildtype controls) when using non-quantitative or semi-quantitative methods to measure $\Delta E3$. We have also highlighted the need to use quantitative methods to limit overestimation of $\Delta E3$ levels, in order to better define the $\Delta E3$ threshold for pathogenicity. We then considered our results in combination with those reported by Tubeuf *et al.* (Tubeuf *et al.*, 2020), with critical examination of the correlation between within-study $\Delta E3$ levels, $\Delta E3$ levels as measured using quantitative dPCR methods in this study, and between-study % survival and results of secondary analysis (Supplementary Table 10). Based on quantitative $\Delta E3$ measurement methods, the combined observations suggest that 56% per-allele expression level of $\Delta E3$ (44% wildtype) for variant c.316+6T>C is sufficient to retain viability (shown by the mESC assay), but ~80% $\Delta E3$ (~20% wildtype) for the c.316+6T>G and c.316+6T>A variants displays across- and within-study discordant results suggestive of hypomorphic effect (and potentially associated with reduced cancer risk). It will be critical to compile additional clinical data to inform classifications of these variants, and in parallel to consider alternative functional assays that may capture more subtle impacts on function.

Independence and application of ACMG/AMP codes, and issues for consideration

We highlight for future discussion issues around independence and application of several ACMG/AMP classification codes. The first question is whether PS3 (Functional studies supportive of damaging effect) should be applied for observation

of mRNA results in addition to a relevant PVS1 code for acceptor or donor site variants. Given the extremely high prior probability that a variant altering the highly conserved donor or acceptor site dinucleotide sequence will have an extensive impact on splicing, confirmation of a well-predicted splicing effect adds little information. For example, if an in-frame predicted splicing event is assigned PVS1_Supporting according to the flowchart of Tayoun et al. (Abou Tayoun et al., 2018), then confirmation of such an in-frame event does not alter the uncertainty around whether the in-frame event is important to protein function. Thus, a conservative approach would be to retain the bioinformatic “PVS1” code when confirmed, and simply denote as “confirmed”. Further, in the unlikely event that a bioinformatic “PVS1” code is shown to contrast with an experimental result, the reason for the contrasting findings should be used to inform specific and general concepts in derivation of gene-specific PVS1 flowcharts. Given that PS3 is also used to assign results from assays of protein function, or survival assays which measure effect on combined mRNA and protein, perhaps it would be simpler to retain PS3 only for application of “functional assays” that capture more than mRNA splicing, since as shown here they can provide additional information to that from mRNA splicing results. The second question is whether it is double-counting to apply PS1(Splicing) on the basis of similarity to prediction for a known pathogenic variant at the same position. We argue not, since the rationale for applying the PS1(Splicing code) is - as for the baseline PS1 missense code - that the clinical information for a pathogenic variant can be “borrowed” as evidence to classify a second variant, for which pathogenicity is assumed to be due to the same molecular

mechanism. The use of a PS1_Splicing code is particularly important for variants outside of the donor and acceptor sites, with a starting bioinformatic code at only supporting level. We also raise for debate whether the same concept should be introduced as a new ACMG/AMP code as evidence against pathogenicity. That is, if a variant with no prediction to alter a missense or splicing profile is classified as benign using clinical and other data, then another variant with the same bioinformatics scores could be assumed also to have no molecular and clinical impact on disease risk. In addition, we show here how missense variant location outside a domain provides valuable evidence against pathogenicity, irrespective of bioinformatic prediction of missense effect. Conceptually this is not new, and has been captured as low prior probability of pathogenicity for *BRCA1* and *BRCA2* multifactorial likelihood analysis analysis (Easton et al., 2007; Li et al., 2020); we assigned this evidence type as BP1_Strong, since it is not captured in the baseline ACMG-AMP criteria.

Conclusions

There were three main messages arising from this study. Firstly, annotation of donor and acceptor sites requires careful consideration of cryptic splice site usage and critical domain knowledge to appropriately assign PVS1 code strength. Secondly, splicing assays have great utility for functional assessment of intronic and synonymous variants, but genomic-based functional assays that capture both mRNA and protein effects provide critical findings for the assessment of variants leading to transcript profiles of uncertain significance, including those encoding a

missense change/s. Thirdly, statistically derived odds and LRs for variant pathogenicity assessment, derived for a range of data types, show great utility in a gene-specific points-based application of ACMG/AMP guidelines.

Web Resources used in this study

<http://varnomen.hgvs.org/>

<https://spliceailookup.broadinstitute.org>

<http://fengbj-laboratory.org/BayesDel/BayesDel.html>

<http://agvgd.hci.utah.edu/>

Acknowledgements

The authors thank J. Jonkers and P. Bouwman (Netherlands Cancer Institute, Amsterdam, the Netherlands) for the I-Sce1-mCherry plasmid; S.K. Sharan (National Cancer Institute at Frederick, Frederick, USA) for the PI2F7 conditional Brca2 knockout mES cell line (PMID: 18607349); M. Jasin (Memorial Sloan-Kettering Cancer Center, New York, USA) for the DR-GFP reporter plasmid (PMID: 11239455). The authors wish also to thank all the members of the ICO Hereditary Cancer Program. LCW was supported by the Royal Society of New Zealand Rutherford Discovery Fellowship. The FPGMX thank members of the Cancer Genetics group (IDIS): Miguel Aguado, Olivia Fuentes, and Ana Crujeiras.

Grant support: The work of MPG was financially supported by the Dutch Cancer Society KWF (UL2012-5649 and Pink Ribbon-11704). The work by PM was supported by a “Pink ribbon” grant #194751 from Den Norske Kreftforening to E.H. The work of MdH was supported by Spanish Instituto de Salud Carlos III (ISCIII) funding grant PI 20/00110, an initiative of the Spanish Ministry of Economy and

Innovation. ABS, MTP and ET were supported by NHMRC Funding (APP177524, APP1104808). The work by CL and MM received institutional support by CERCA Program/ Generalitat de Catalunya and grant support by the Carlos III National Health Institute funded by FEDER funds – a way to build Europe – [PI19/00553; PI16/00563; SAF2015-68016-R and CIBERONC]; the Government of Catalonia [Pla estratègic de recerca i innovació en salut (PERIS_MedPerCan and URDCat projects), 2017SGR1282 and 2017SGR496]. The Baralle lab is supported by NIHR Research Professorship to DB (RP-2016-07- 011). The work of AV was supported by the Spanish Health Research Foundation, Instituto de Salud Carlos III (ISCIII) through Research Activity Intensification Program (contract grant numbers: INT15/00070, INT16/00154, INT17/00133, INT20/00071), and through Centro de Investigación Biomédica en Red de Enfermedades Raras CIBERER (ACCI 2016: ER17P1AC7112/2018); Autonomous Government of Galicia (Consolidation and structuring program: IN607B), and by the Fundación Mutua Madrileña (call 2018). The German Consortium of Hereditary Breast and Ovarian Cancer (GC-HBOC) is supported by the German Cancer Aid (grant no 110837 and 70114178), (RKS) and by the Federal Ministry of Education and Research (grant no 01GY1901), (RKS). The work of EMA was Supported by Ministry of Health of the Czech Republic MH CZ – DRO (MMCI, 00209805) and AZV project NU20-03-00285. Institutional support by Italian Ministry of Health, Ricerca Corrente of CRO Aviano, Line 1 (AVI).

Conflict Of Interest

The PERCH software, for which BJ Feng is the inventor, has been non-exclusively licensed to Ambry Genetics Corporation for their clinical genetic testing services and research. Dr. Feng also reports funding and sponsorship to his institution on his behalf from Pfizer Inc., Regeneron Genetics Center LLC., and Astra Zeneca. TvOH has received lecture honoraria from Pfizer. Nelly Abualkheir, Blair R. Conner, Lily Hoang, Rachid Karam, Holly LaDuca, Tina Pesaran, and Marcy E. Richardson are paid employees of Ambry Genetics. All other authors have declared no conflicts of interest.

Data availability

All summary results and sources are provided in the Supplementary Tables. More detailed data e.g. pedigree structures and segregation information, and reported family history data, are not publicly available due to ethical restrictions. All variants in the project have been submitted to the LOVD3 database.

Figure legends

Figure 1

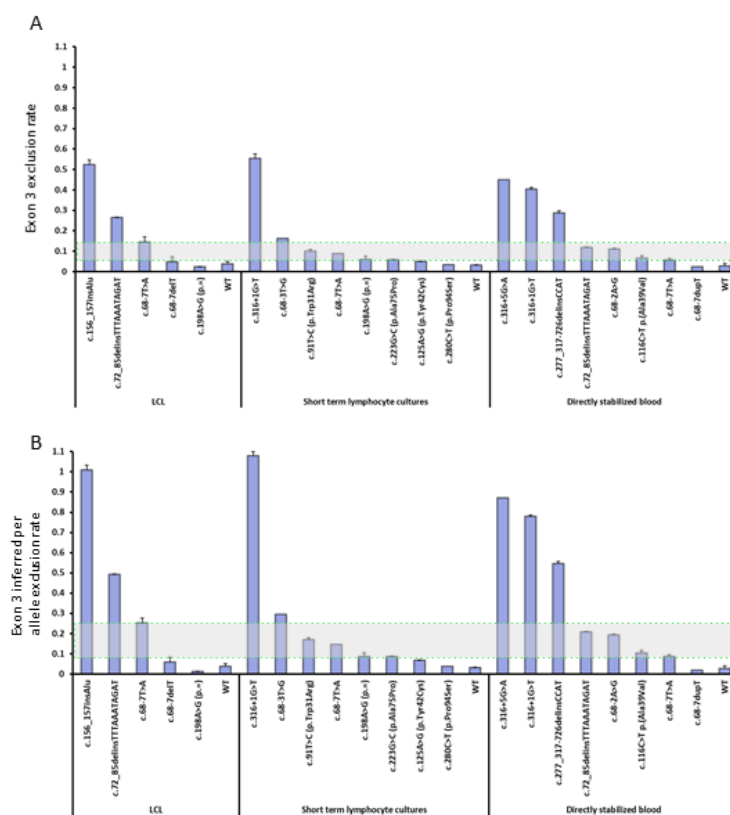


Figure 1.

Quantitative dPCR of $\Delta E3$ in patient samples. A. Measured (absolute) $\Delta E3$ rate.

B. Inferred per-allele $\Delta E3$ rate. See methods for details about $\Delta E3$ rate calculations.

Three different sample types were analyzed: lymphoblastoid cell line cultures (LCL), short term lymphocyte cultures, and directly stabilized blood (Paxgene, Tempus, Trizol). Mean values and standard deviation for at least 2 replicates for each variant are shown. Complete $\Delta E3$ variant controls are c.156_157insAlu and c.316+5G>A.

The $\Delta E3$ rate interval for known benign variant c.68-7T>A is shown as a horizontal green bar, defined by the lower boundary observed for RNA from directly stabilized blood and the upper boundary observed for RNA from LCL culture.

Figure 2

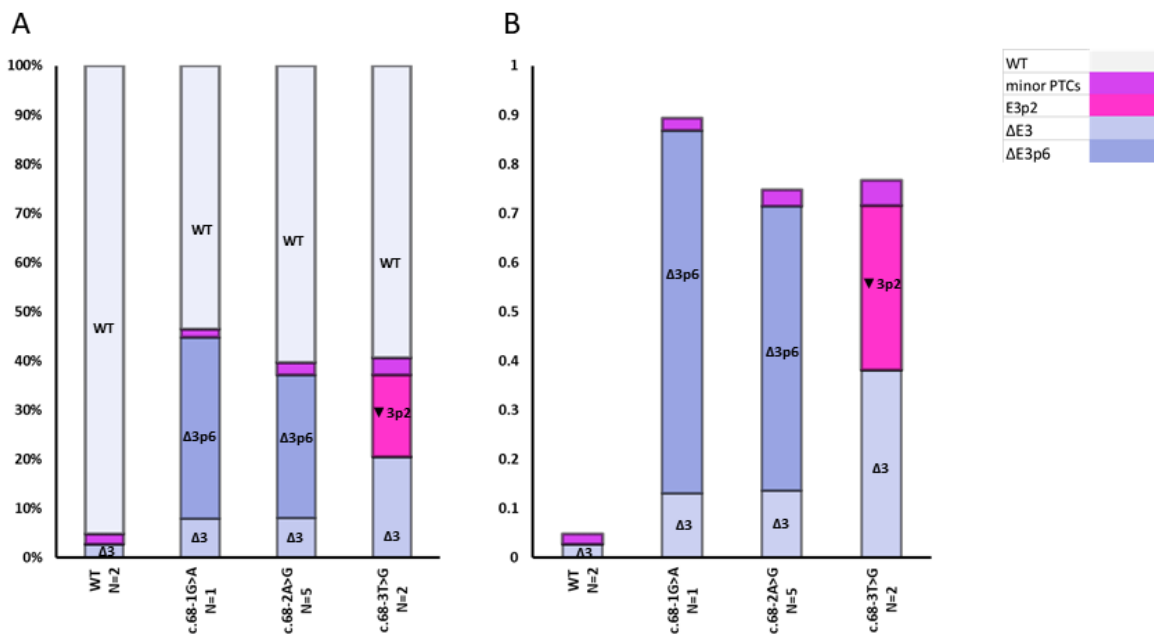


Figure 2.

Quantitative RNA sequencing of patient RNA samples. A) Relative contribution of transcripts (expressed as a proportion of total 100%). B) The bars show inferred per-allele expression relative to total transcript amount. A number of low expressed transcripts expected to encode a protein termination codon (PTC) are summarized

as minor PTCs. More detailed information, including standard deviation measures, is available in Figure S6a. N = number of individuals assayed.

Figure 3

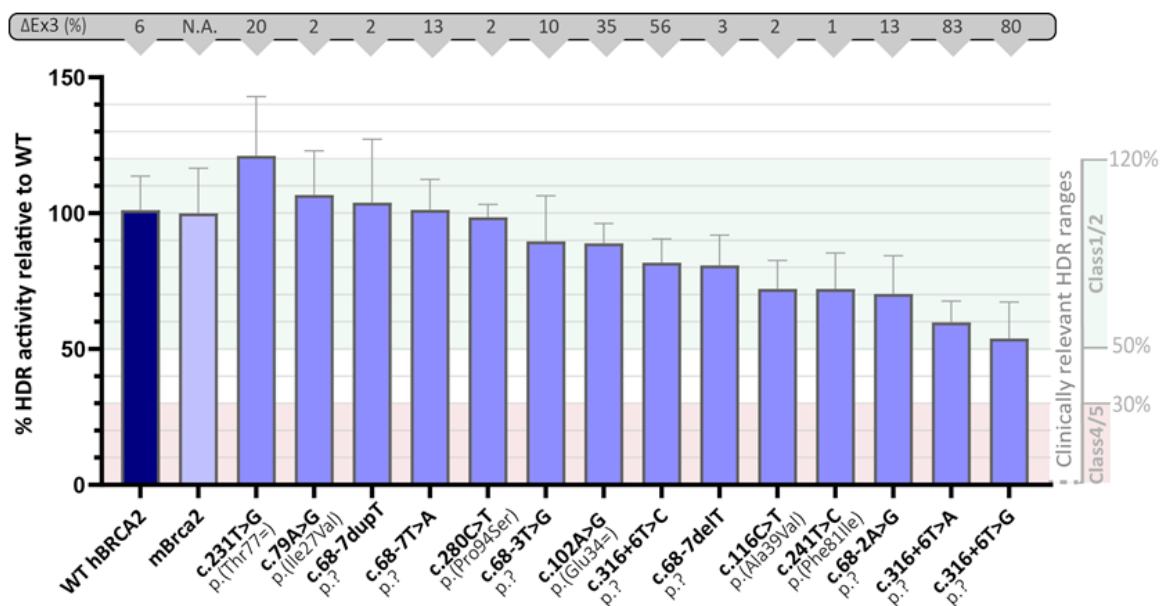


Figure 3.

HDR activity of *BRCA2* exon 3 variants in mESC. The fraction of GFP-expressing cells was determined by flow cytometry two days post-transfection with an I-Sce1 expression vector. *mBrca2* represents the conditional *Brca2*^{-loxP}; Pim1^{DR-GFP/WT} cell line expressing endogenous mouse *Brca2*. The upper green box represents the HDR range previously reported for Class 1/2 *BRCA2* variants (classified as (likely)

benign using multifactorial likelihood analysis). The lower red box represents the HDR range reported to be associated with >95% probability of pathogenicity (Guidugli et al., 2018), and used to define a pathogenic HDR range for the mESC assay (Mesman et al., 2019). Error bars indicate the SD of at least six independent GFP measurements per variant. The upper grey bar indicates the $\Delta E3$ levels as measured by quantitative dPCR (E2E4 junctions vs. E3E4 junctions) using RNA samples isolated from variant-expressing mESC. Note that E3E4 junction captures full-length expression, but also expression of $\nabla E3p2$ and $\Delta E3p6$ transcripts (as observed respectively, in c.68-3T>G and c.68-2A>G mESCs).

Figure 4

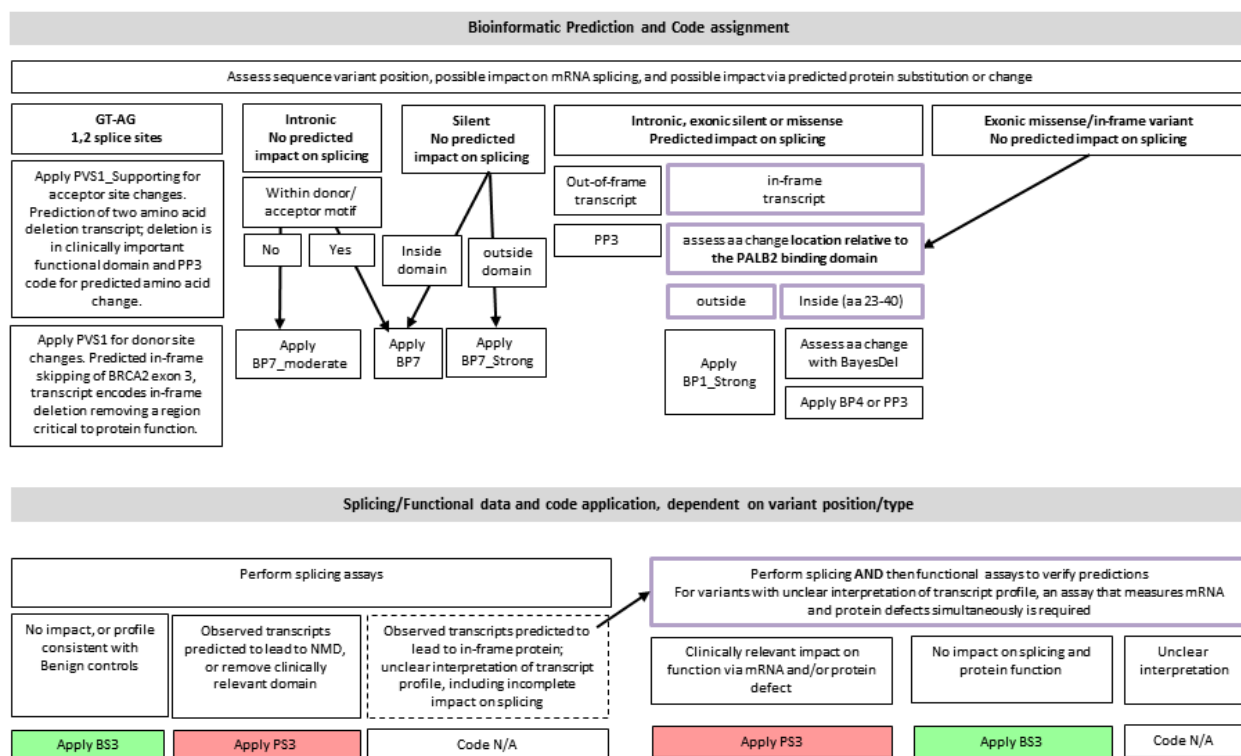


Figure 4

Application of codes for variant location relative to functional domain, bioinformatic prediction of effect, and mRNA and/or protein assay data, as applied to variants in/near *BRCA2* exon 3. The donor/acceptor motif location was derived from that of Cartegni et al (Cartegni et al., 2002), namely up to and including the +8 position for the donor motif, and up to and including the -12 position for the acceptor site motif. The PALB2 interaction domain contained within exon 3 was designated conservatively as amino acids (aa) 23-40. Purple border designates variant for which both splicing and functional data is required to consider

assignment of BS3 or PS3 codes. Refer to methods section for more detail on level of mRNA aberration and/or functional impact used to assign these codes.

References

- Abou Tayoun, A. N., Pesaran, T., DiStefano, M. T., Oza, A., Rehm, H. L., Biesecker, L. G.,... ClinGen Sequence Variant Interpretation Working, G. (2018). Recommendations for interpreting the loss of function PVS1 ACMG/AMP variant criterion. *Hum Mutat*, 39(11), 1517-1524. doi:10.1002/humu.23626
- Biswas, K., Das, R., Eggington, J. M., Qiao, H., North, S. L., Stauffer, S.,... Sharan, S. K. (2012). Functional evaluation of BRCA2 variants mapping to the PALB2-binding and C-terminal DNA-binding domains using a mouse ES cell-based assay. *Hum Mol Genet*, 21(18), 3993-4006. doi:10.1093/hmg/dds222
- Breast Cancer Association, C., Dorling, L., Carvalho, S., Allen, J., Gonzalez-Neira, A., Luccarini, C.,... Easton, D. F. (2021). Breast Cancer Risk Genes - Association Analysis in More than 113,000 Women. *N Engl J Med*, 384(5), 428-439. doi:10.1056/NEJMoa1913948
- Canson, D., Glubb, D., & Spurdle, A. B. (2020). Variant effect on splicing regulatory elements, branchpoint usage, and pseudoexonization: Strategies to enhance bioinformatic prediction using hereditary cancer genes as exemplars. *Hum Mutat*, 41(10), 1705-1721. doi:10.1002/humu.24074
- Caputo, S. M., Leone, M., Damiola, F., Ehlen, A., Carreira, A., Gaidrat, P.,... Rouleau, E. (2018). Full in-frame exon 3 skipping of BRCA2 confers high risk of breast and/or ovarian cancer. *Oncotarget*, 9(25), 17334-17348. doi:10.18632/oncotarget.24671
- Caputo, S. M., Telly, D., Briaux, A., Sesen, J., Ceppi, M., Bonnet, F.,... Rouleau, E. (2021). 5' Region Large Genomic Rearrangements in the BRCA1 Gene in French Families:

- Identification of a Tandem Triplication and Nine Distinct Deletions with Five Recurrent Breakpoints. *Cancers (Basel)*, 13(13). doi.org/10.3390/cancers13133171
- Cartegni, L., Chew, S. L., & Krainer, A. R. (2002). Listening to silence and understanding nonsense: exonic mutations that affect splicing. *Nat Rev Genet*, 3(4), 285-298. doi:10.1038/nrg775
- Colombo, M., Lopez-Perolio, I., Meeks, H. D., Caleca, L., Parsons, M., Li, H.,... Radice, P. (2018). The BRCA2 c.68-7T > A variant is not pathogenic: A model for clinical calibration of spliceogenicity. *Hum Mutat*. doi:10.1002/humu.23411
- Conner, B. R., Hernandez, F., Souders, B., Landrith, T., Boland, C. R., & Karam, R. (2019). RNA Analysis Identifies Pathogenic Duplications in MSH2 in Patients With Lynch Syndrome. *Gastroenterology*, 156(6), 1924-1925 e1924. doi:10.1053/j.gastro.2019.01.248
- de Garibay, G. R., Acedo, A., Garcia-Casado, Z., Gutierrez-Enriquez, S., Tosar, A., Romero, A.,... de la Hoya, M. (2014). Capillary electrophoresis analysis of conventional splicing assays: IARC analytical and clinical classification of 31 BRCA2 genetic variants. *Hum Mutat*, 35(1), 53-57. doi.org/10.1002/humu.22456
- de la Hoya, M., Soukarieh, O., Lopez-Perolio, I., Vega, A., Walker, L. C., van Ierland, Y.,... Spurdle, A. B. (2016). Combined genetic and splicing analysis of BRCA1 c.[594-2A>C; 641A>G] highlights the relevance of naturally occurring in-frame transcripts for developing disease gene variant classification algorithms. *Hum Mol Genet*, 25(11), 2256-2268. doi:10.1093/hmg/ddw094
- Diez, O., Gutierrez-Enriquez, S., Ramon y Cajal, T., Alonso, C., Balmana, J., & Llorca, G. (2007). Caution should be used when interpreting alterations affecting the exon 3 of the BRCA2 gene in breast/ovarian cancer families. *J Clin Oncol*, 25(31), 5035-5036; author reply 5036-5038. doi:10.1200/JCO.2007.13.4346

- Dines, J. N., Shirts, B. H., Slavin, T. P., Walsh, T., King, M. C., Fowler, D. M., & Pritchard, C. C. (2020). Systematic misclassification of missense variants in BRCA1 and BRCA2 “coldspots”. *Genetics in Medicine*, 22(5), 825-830. doi:10.1038/s41436-019-0740-6
- Easton, D. F., Deffenbaugh, A. M., Pruss, D., Frye, C., Wenstrup, R. J., Allen-Brady, K.,... Goldgar, D. E. (2007). A systematic genetic assessment of 1,433 sequence variants of unknown clinical significance in the BRCA1 and BRCA2 breast cancer-predisposition genes. *Am J Hum Genet*, 81(5), 873-883. doi:10.1086/521032
- Fackenthal, J. D., Yoshimatsu, T., Zhang, B., de Garibay, G. R., Colombo, M., De Vecchi, G.,... de la Hoya, M. (2016). Naturally occurring BRCA2 alternative mRNA splicing events in clinically relevant samples. *J Med Genet*, 53(8), 548-558. doi:10.1136/jmedgenet-2015-103570
- Farber-Katz, S., Hsuan, V., Wu, S., Landrith, T., Vuong, H., Xu, D.,... Karam, R. (2018). Quantitative Analysis of BRCA1 and BRCA2 Germline Splicing Variants Using a Novel RNA-Massively Parallel Sequencing Assay. *Front Oncol*, 8, 286. doi:10.3389/fonc.2018.00286
- Fraile-Bethencourt, E., Valenzuela-Palomo, A., Diez-Gomez, B., Goina, E., Acedo, A., Buratti, E., & Velasco, E. A. (2019). Mis-splicing in breast cancer: identification of pathogenic BRCA2 variants by systematic minigene assays. *J Pathol*, 248(4), 409-420. doi:10.1002/path.5268
- Gayther, S. A., Mangion, J., Russell, P., Seal, S., Barfoot, R., Ponder, B. A.,... Easton, D. (1997). Variation of risks of breast and ovarian cancer associated with different germline mutations of the BRCA2 gene. *Nat Genet*, 15(1), 103-105. doi:10.1038/ng0197-103

- Goldgar, D. E., Easton, D. F., Byrnes, G. B., Spurdle, A. B., Iversen, E. S., Greenblatt, M. S., & Group, I. U. G. V. W. (2008). Genetic evidence and integration of various data sources for classifying uncertain variants into a single model. *Hum Mutat*, *29*(11), 1265-1272. doi:10.1002/humu.20897
- Goldgar, D. E., Easton, D. F., Deffenbaugh, A. M., Monteiro, A. N., Tavtigian, S. V., Couch, F. J., & Breast Cancer Information Core Steering, C. (2004). Integrated evaluation of DNA sequence variants of unknown clinical significance: application to BRCA1 and BRCA2. *Am J Hum Genet*, *75*(4), 535-544. doi:10.1086/424388
- Guidugli, L., Shimelis, H., Masica, D. L., Pankratz, V. S., Lipton, G. B., Singh, N.,... Couch, F. J. (2018). Assessment of the Clinical Relevance of BRCA2 Missense Variants by Functional and Computational Approaches. *Am J Hum Genet*. doi:10.1016/j.ajhg.2017.12.013
- Hartford, S. A., Chittela, R., Ding, X., Vyas, A., Martin, B., Burkett, S.,... Sharan, S. K. (2016). Interaction with PALB2 Is Essential for Maintenance of Genomic Integrity by BRCA2. *PLoS Genet*, *12*(8), e1006236. doi:10.1371/journal.pgen.1006236
- Ikegami, M., Kohsaka, S., Ueno, T., Momozawa, Y., Inoue, S., Tamura, K.,... Mano, H. (2020). High-throughput functional evaluation of BRCA2 variants of unknown significance. *Nat Commun*, *11*(1), 2573. doi:10.1038/s41467-020-16141-8
- Jaganathan, K., Kyriazopoulou Panagiotopoulou, S., McRae, J. F., Darbandi, S. F., Knowles, D., Li, Y. I.,... Farh, K. K. (2019). Predicting Splicing from Primary Sequence with Deep Learning. *Cell*, *176*(3), 535-548 e524. doi:10.1016/j.cell.2018.12.015
- Landrith, T., Li, B., Cass, A. A., Conner, B. R., LaDuca, H., McKenna, D. B.,... Karam, R. (2020). Splicing profile by capture RNA-seq identifies pathogenic germline variants in tumor suppressor genes. *NPJ Precis Oncol*, *4*, 4. doi:10.1038/s41698-020-0109-y

- Li, H., LaDuca, H., Pesaran, T., Chao, E. C., Dolinsky, J. S., Parsons, M.,... Goldgar, D. E. (2020). Classification of variants of uncertain significance in BRCA1 and BRCA2 using personal and family history of cancer from individuals in a large hereditary cancer multigene panel testing cohort. *Genetics in Medicine*, 22(4), 701-708. doi:10.1038/s41436-019-0729-1
- Mesman, R. L. S., Calleja, F., de la Hoya, M., Devilee, P., van Asperen, C. J., Vrieling, H., & Vreeswijk, M. P. G. (2020). Alternative mRNA splicing can attenuate the pathogenicity of presumed loss-of-function variants in BRCA2. *Genetics in Medicine*, 22(8), 1355-1365. doi:10.1038/s41436-020-0814-5
- Mesman, R. L. S., Calleja, F. M. G. R., Hendriks, G., Morolli, B., Misovic, B., Devilee, P.,... Vreeswijk, M. P. G. (2019). The functional impact of variants of uncertain significance in BRCA2. *Genetics in Medicine*, 21(2), 293-302. doi:10.1038/s41436-018-0052-2
- Mohammadi, L., Vreeswijk, M. P., Oldenburg, R., van den Ouweland, A., Oosterwijk, J. C., van der Hout, A. H.,... van Houwelingen, H. C. (2009). A simple method for co-segregation analysis to evaluate the pathogenicity of unclassified variants; BRCA1 and BRCA2 as an example. *BMC Cancer*, 9, 211. doi:10.1186/1471-2407-9-211
- Montalban, G., Fraile-Bethencourt, E., Lopez-Perolio, I., Perez-Segura, P., Infante, M., Duran, M.,... Gutierrez-Enriquez, S. (2018). Characterization of spliceogenic variants located in regions linked to high levels of alternative splicing: BRCA2 c.7976+5G > T as a case study. *Hum Mutat*, 39(9), 1155-1160. doi.org/10.1002/humu.23583
- Nacson, J., Di Marcantonio, D., Wang, Y., Bernhardt, A. J., Clausen, E., Hua, X.,... Johnson, N. (2020). BRCA1 Mutational Complementation Induces Synthetic Viability. *Mol Cell*, 78(5), 951-959 e956. doi:10.1016/j.molcel.2020.04.006

- Nix, P., Mundt, E., Coffee, B., Goossen, E., Warf, B. M., Brown, K.,... Roa, B. (2021). Interpretation of BRCA2 Splicing Variants: A Case Series of Challenging Variant Interpretations and the Importance of Functional RNA Analysis. *Fam Cancer*. doi:10.1007/s10689-020-00224-y
- Nordling, M., Karlsson, P., Wahlstrom, J., Engwall, Y., Wallgren, A., & Martinsson, T. (1998). A large deletion disrupts the exon 3 transcription activation domain of the BRCA2 gene in a breast/ovarian cancer family. *Cancer Res*, 58(7), 1372-1375.
- Oliver, A. W., Swift, S., Lord, C. J., Ashworth, A., & Pearl, L. H. (2009). Structural basis for recruitment of BRCA2 by PALB2. *EMBO Rep*, 10(9), 990-996. doi:10.1038/embor.2009.126
- Parsons, M. T., Tudini, E., Li, H., Hahnen, E., Wappenschmidt, B., Feliubadalo, L.,... Spurdle, A. B. (2019). Large scale multifactorial likelihood quantitative analysis of BRCA1 and BRCA2 variants: An ENIGMA resource to support clinical variant classification. *Hum Mutat*, 40(9), 1557-1578. doi:10.1002/humu.23818
- Peixoto, A., Santos, C., Rocha, P., Pinheiro, M., Principe, S., Pereira, D.,... Teixeira, M. R. (2009). The c.156_157insAlu BRCA2 rearrangement accounts for more than one-fourth of deleterious BRCA mutations in northern/central Portugal. *Breast Cancer Res Treat*, 114(1), 31-38. doi:10.1007/s10549-008-9978-4
- Richards, S., Aziz, N., Bale, S., Bick, D., Das, S., Gastier-Foster, J.,... Committee, A. L. Q. A. (2015). Standards and guidelines for the interpretation of sequence variants: a joint consensus recommendation of the American College of Medical Genetics and Genomics and the Association for Molecular Pathology. *Genetics in Medicine*, 17(5), 405-424. doi:10.1038/gim.2015.30
- Sanz, D. J., Acedo, A., Infante, M., Duran, M., Perez-Cabornero, L., Esteban-Cardenosa, E.,... Velasco, E. A. (2010). A high proportion of DNA variants of BRCA1 and

BRCA2 is associated with aberrant splicing in breast/ovarian cancer patients. *Clin Cancer Res*, 16(6), 1957-1967. doi:10.1158/1078-0432.CCR-09-2564

Shamsani, J., Kazakoff, S. H., Armean, I. M., McLaren, W., Parsons, M. T., Thompson, B. A.,... Spurdle, A. B. (2019). A plugin for the Ensembl Variant Effect Predictor that uses MaxEntScan to predict variant spliceogenicity. *Bioinformatics*, 35(13), 2315-2317. doi:10.1093/bioinformatics/bty960

Spurdle, A. B., Couch, F. J., Parsons, M. T., McGuffog, L., Barrowdale, D., Bolla, M. K.,... kConFab, I. (2014). Refined histopathological predictors of BRCA1 and BRCA2 mutation status: a large-scale analysis of breast cancer characteristics from the BCAC, CIMBA, and ENIGMA consortia. *Breast Cancer Res*, 16(6), 3419. doi:10.1186/s13058-014-0474-y

Spurdle, A. B., Healey, S., Devereau, A., Hogervorst, F. B., Monteiro, A. N., Nathanson, K. L.,... Enigma. (2012). ENIGMA--evidence-based network for the interpretation of germline mutant alleles: an international initiative to evaluate risk and clinical significance associated with sequence variation in BRCA1 and BRCA2 genes. *Hum Mutat*, 33(1), 2-7. doi:10.1002/humu.21628

Sy, S. M., Huen, M. S., & Chen, J. (2009). PALB2 is an integral component of the BRCA complex required for homologous recombination repair. *Proc Natl Acad Sci U S A*, 106(17), 7155-7160. doi:10.1073/pnas.0811159106

Tavtigian, S. V., Byrnes, G. B., Goldgar, D. E., & Thomas, A. (2008). Classification of rare missense substitutions, using risk surfaces, with genetic- and molecular-epidemiology applications. *Hum Mutat*, 29(11), 1342-1354. doi:10.1002/humu.20896

Tavtigian, S. V., Greenblatt, M. S., Harrison, S. M., Nussbaum, R. L., Prabhu, S. A., Boucher, K. M.,... ClinGen Sequence Variant Interpretation Working, G. (2018). Modeling the ACMG/AMP variant classification guidelines as a Bayesian

classification framework. *Genetics in Medicine*, 20(9), 1054-1060.
doi:10.1038/gim.2017.210

Tavtigian, S. V., Harrison, S. M., Boucher, K. M., & Biesecker, L. G. (2020). Fitting a naturally scaled point system to the ACMG/AMP variant classification guidelines. *Hum Mutat*. doi:10.1002/humu.24088

Thomassen, M., Blanco, A., Montagna, M., Hansen, T. V., Pedersen, I. S., Gutierrez-Enriquez, S.,... Vega, A. (2012). Characterization of BRCA1 and BRCA2 splicing variants: a collaborative report by ENIGMA consortium members. *Breast Cancer Res Treat*, 132(3), 1009-1023. doi:10.1007/s10549-011-1674-0

Thompson, D., Easton, D. F., & Goldgar, D. E. (2003). A full-likelihood method for the evaluation of causality of sequence variants from family data. *Am J Hum Genet*, 73(3), 652-655. doi:10.1086/378100

Tubeuf, H., Caputo, S. M., Sullivan, T., Rondeaux, J., Krieger, S., Caux-Moncoutier, V.,... Martins, A. (2020). Calibration of Pathogenicity Due to Variant-Induced Leaky Splicing Defects by Using BRCA2 Exon 3 as a Model System. *Cancer Res*, 80(17), 3593-3605. doi:10.1158/0008-5472.CAN-20-0895

Valenzuela-Palomo, A., Bueno-Martinez, E., Sanoguera-Miralles, L., Lorca, V., Fraile-Bethencourt, E., Esteban-Sanchez, A.,... Velasco, E. A. (2022). Splicing predictions, minigene analyses, and ACMG-AMP clinical classification of 42 germline PALB2 splice-site variants. *J Pathol*, 256(3), 321-334. doi.org/10.1002/path.5839

Xia, B., Sheng, Q., Nakanishi, K., Ohashi, A., Wu, J., Christ, N.,... Livingston, D. M. (2006). Control of BRCA2 cellular and clinical functions by a nuclear partner, PALB2. *Mol Cell*, 22(6), 719-729. doi:10.1016/j.molcel.2006.05.022

Yeo, G., & Burge, C. B. (2004). Maximum entropy modeling of short sequence motifs with applications to RNA splicing signals. *J Comput Biol*, 11(2-3), 377-394.
doi:10.1089/1066527041410418

Table 1: Summary of mRNA and/or functional studies conducted as part of this study†

Variant	Protein	Mini gene [§]	Patient RNA					mESC assay			Classification based on all information collated to date, using gene-specific ACMG /AMP criteria and points system approach.
			Splice assay using patient samples [§]	dPCR absolute exclusion rate [§]	dPCR inferred per-allele exclusion rate	RNA sequencing transcript proportions [§]	RNA sequencing inferred per-allele transcript proportions	dPCR absolute per-allele $\Delta(E3)$ exclusion rate [§]	Complementation Category* <small>(clone stability: poor, <20%; reduced, 20-50%; good, >50%)</small>	HD R capacity (%)	
WT	N/A	Reference	$\Delta E3 \uparrow$ (Blood, Lymphocyte, LCL)	2.8% (Blood), 3.1% (Lymphocyte), 3.7% (LCLs)	N/A	$\Delta(E3)$ 2.7% (2.4-3.0%)(Blood)	$\Delta(E3)$ 2.7% (2.4-3.0%)(Blood)	6.1%	Ref	Ref	N/A
c.68-7T>A	p.?	$\Delta E3 \uparrow$, 7% skipping reported in Caputo et al (PMID 29707112)	$\Delta E3 \uparrow \uparrow$, reported in Colombo et al (PMID:29460995)	5.7% (Blood), 8.9% (Lymphocyte), 14.5% (LCLs)	8.7% (Blood), 14.7% (Lymphocyte), 25.2% (LCLs)			13.3%	Good	101	Partial skipping control - established Benign variant
c.156_157insAlu	p.?		$\Delta E3 \uparrow \uparrow \uparrow$ (LCL)	52.3% (LCL)	100.0% (LCL)						Full skipping control - established

											hed Pathogenic Variant
c.316+5G>C	p.?	$\Delta E3 \uparrow \uparrow \uparrow$, 95% exon skipping reported in Caputo et al (PMID 2970 7112)						99.1%	Poor	NA	Full skipping control - established Pathogenic variant
c.316+5G>A	p.?	$\Delta E3 \uparrow \uparrow \uparrow$, 94% exon skipping reported in Caputo et al (PMID 2970 7112)	$\Delta E3 \uparrow \uparrow \uparrow$ (Blood)	44.9% (Blood)	87.0% (Blood)						Full skipping control - confirmed as pathogenic based on ACMG /AMP approach, this study
c.231T>G	p.(=)							19.9%	Good	121	Partial skipping control - Benign control based on frequency, previous mESC results - selected as control for mESC assays in this study
c.68-7delT	p.?		$\Delta E3 \uparrow \uparrow$ (LCL)	4.9% (LCL)	6.0% (LCL)			2.5%	Good	81	Likely Benign
c.68-7dupT	p.?	$\Delta E3 \uparrow$	same as WT (Lymphocyte)	2.3% (Blood)	1.9% (Blood)			2.0%	Good	104	Benign
c.68-3T>G	p.?	$\Delta E3 \uparrow \uparrow$		16.3% (Lymphocyte)	29.7% (Lymphocyte)	$\Delta(E3)$, 20.4% (19.0-21.9%); $\Delta(E3-E4)$, 2.4% (2.2-	$\Delta(E3)$, 38.1 (35.2-41.1%); $\Delta(E3-$	9.9%	Good	90	Benign

						2.6%); ▼(E3p2), 16.7% (14.5-19.0%)	E4, 4.3% (4.0-4.7%); ▼(E3p2), 33.4% (29.0-37.8%).					
c.68-2A>C	p.?	Δ(E3p6)										Uncertain
c.68-2A>T	p.?	Δ(E3p6)										Uncertain
c.68-2A>G	p.?	ΔE3↑, Δ(E3p6)	Δ(E3p6) (blood)	11.1% (Blood)	19.4% (Blood)	Δ(E3p6), 28.9% (26.0-31.1%); Δ(E3), 8.2% (6.6-10.2%)	Δ(E3p6), 57.9% (52.0-62.2%); Δ(E3), 13.6% (10.4-17.6%)	12.8%	Good	70		Likely Benign
c.68-1G>A	p.?	ΔE3↑, Δ(E3p6)				Δ(E3p6), 36.8%; Δ(E3), 7.9%	Δ(E3p6), 73.6%; Δ(E3), 13.2%					Uncertain
c.68-1G>C	p.?	Δ(E3p6)										Uncertain
c.68-1G>T	p.?	Δ(E3p6)										Uncertain
c.72_85delinsTTAAATAGAT	p.(Leu24_Leu29delinsPheLeuAsnArgPhe)		ΔE3↑↑, (p.Leu24_Leu29delinsPheLeuAsnArgPhe) (LCL)	26.4% (LCL), 12.0% (Blood)	49.2% (LCL), 20.8% (Blood)			23.5%	Poor	NA		Pathogenic
c.79A>G	p.(Ile27Val)	ΔE3↑						2.0%	Good	107		Likely Benign
c.91T>C	p.(Trp31Arg)	ΔE3↑↑	same as WT (Lymphocytes)	10.1% (Lymphocyte)	17.1% (Lymphocyte)			9.5%	Poor	NA		Likely Pathogenic
c.91T>G	p.(Trp31Gly)							12.0%	Poor	NA		Uncertain
c.93G>C	p.(Trp31Cys)	ΔE3↑↑						10.5%	Poor	NA		Uncertain
c.93G>T	p.(Trp31Cys)							23.3%	Poor	NA		Uncertain
c.102A>G	p.(=)							35.0%	Good	89		Likely Benign
c.116C>T	p.(Ala39Val)	same as WT	same as WT (Blood)	6.6% (Blood)	10.4% (Blood)			2.1%	Good	72		Benign
c.125A>G	p.(Tyr42Cys)	same as WT	same as WT (Lymphocytes)	5.0% (Lymphocyte)	6.9% (Lymphocyte)							Benign

c.167A>C	p.(Asn56Thr)	same as WT										Benign
c.179A>G	p.(Asn60Ser)	same as WT										Benign
c.198A>G	p.(=)	same as WT	same as WT (Lymphocytes)	6.0% (Lymphocyte)	8.9% (Lymphocyte)							Benign
c.223G>C	p.(Ala75Pro)	same as WT	same as WT (Blood, LCL)	5.9% (Lymphocyte)	8.7% (Lymphocyte)							Benign
c.226T>C	p.(Ser76Pro)	ΔE3↑										Likely Benign
c.241T>C	p.(Phe81Ile)	same as WT						0.6%	Good	72		Benign
c.277_317-726delinsCCAT	p.?		ΔE3↑↑↑↑ (Blood)	28.7% (Blood)	54.6% (Blood)							Pathogenic
c.280C>T	p.(Pro94Ser)		same as WT (LCL)	3.5% (LCL)	3.3% (LCL)			1.5%	Good	98		Benign
c.316+1G>T	p.?	ΔE3↑↑↑, complete skipping also reported in Caputo et al (PMID: 29707112)	ΔE3↑↑↑↑ (Lymphocytes)	40.4% (Blood) 55.0% (Lymphocyte)	77.9% (Blood) 107.9% (Lymphocyte)			99.7%	Poor	NA		Pathogenic
c.316+6T>A	p.?							82.6%	Good	60		Uncertain
c.316+6T>G	p.?							80.4%	Reduced	51		Uncertain
c.316+6T>C	p.?							56.3%	Good	82		Likely Benign
c.316+65A>G	p.?	ΔE3↑↑	same as WT (LCL)									Likely Benign

†) Light grey highlighted cell indicates not assayed in this study, for the relevant column. Control samples are in bold.

‡) Transcript notations are as follows: ▼(E3p2) r.67_68ins68-2_68-1 p.(Asp23Gluufs*3); Δ(E3p6) r.68_73del p.(Asp23_Leu24del); Δ(E3) r.68_316del p.(Asp23_Leu105del); Δ(E3_E4) r.68_425del p.(Asp23Valfs*10)

§) Most relevant MES predictions are indicated, with some additional ESE score changes as relevant. For further details about splicing predictions, see Supplementary Table 1. N:0 - no relevant changes predicted at native sites

§) Key to result description: Same as WT - either no skipping, or skipping consistent with WT control/s for assay type; ΔE[↑]: extremely low exon skipping detected by visual inspection but considered greater than WT control variant; ΔE3[↑]: Less than ~10% exon skipping detected by visual inspection; ΔE3[↑↑] exon skipping >10% but considered incomplete by visual inspection.; ΔE3[↑↑↑] (almost) complete skipping. # note that in addition to ΔE3[↑], the variant allele produces an altered full-length transcript r.72_85delinsTTTAAATAGAT p.(Leu24_Leu29delinsPheLeuAsnArgPhe). Multi-exon exclusion was measured by dPCR on patient-derived mRNA for control variants and c.315+1G>T (See Supplementary Figure S4), and was found to occur at negligible levels. Note: Assay on patient mRNA for c.68-2A>G was designed to capture only acceptor site usage, and could not capture upregulation of exon 3 skipping.

¶ Blood = directly stabilized blood, LCL = lymphoblastoid cell line, lymphocyte = short-term lymphocyte culture.

‡) Details listed for alternative transcripts comprising at least 2% of the overall profile. See Supplementary figure S5a for further details about other minor transcripts reported.

‡) Additional notes regarding transcripts detected by capillary electrophoresis (Supplementary Figure S7):

For variant c. 68-3T>G, 10% ΔE3 transcript was expressed relative to full-length plus ▼(E3p2) transcripts.

For variant c. 68-2A>G, no full-length transcript was detected, only exon skipping and a 6bp deletion transcript consistent with predicted cryptic site usage; 13% ΔE3 transcript was expressed relative to Δ(E3p6) transcript (r.68_73del).

*) Complementation categories were defined based on clone viability relative to wildtype, as follows: poor (<20% viability), reduced (20-50% viability) and good (>50% viability).

Blue font: exon 3 exclusion at levels considered clinically unimportant (if no other impact on mRNA splicing), including: not detectable, at low levels comparable to wildtype, similar to that of benign control c.68-7T>A, or estimated from quantitative studies to be at or below 30% inferred per-allele $\Delta E3$).

Accepted Article